doi:10.6041/j.issn.1000-1298.2016.01.015

Design and Performance Analysis of Composite Sensor for Multilayer Soil Profile

Gao Zhitao[1,2] Liu Weiping[1,2] Zhao Yandong[1,2] Zhang Chaoyi[1,2]

(1. *School of Technology*, *Beijing Forestry University*, *Beijing* 100083, *China*
2. *Beijing Laboratory of Urban and Rural Ecological Environment*, *Beijing Forestry University*, *Beijing* 100083, *China*)

Abstract: Considering the many difficulties of installing the sensor for the soil temperature and moisture measurement, such as miserable installation of the sensor and relatively large disturbance to the local soil, this paper designed a composite sensor for multilayer soil profile in accordance with the principles of soil moisture measurement and temperature measurement based on SWR and platinum resistance. A vector network analyzer and HFSS electromagnetic simulation software were used to analyze impedance characteristic and electric field distribution of the sensor electrode. According to the analysis result, the structure of copper detection probe was designed. The diameter of the probe is 5 cm, the width is 2.5 cm, the thickness is 0.09 cm and the excitation frequency of test circuit is 100 MHz. Three types of soil were chose as experimental samples. The polynomial fitting and linear fitting were conducted on the output values of sensor detection unit. The results correlation reached more than 0.99. The static and dynamic performance of the system met the detection requirements of temperature and moisture of soil profile. Experiments was carried out in Xiaotangshan District, Beijing City, and then effect of temperature and volumetric moisture content of soil on sensor outputs were analyzed and correction models were established by using the statistical regression method at different temperatures. The sensor working in the PVC pipe buried in the soil could obtain the information of temperature and moisture of the three layers, and its performance was stable and the data was reliable. This study provides a highly efficient method for obtaining the real - time information of multilayer soil moisture and temperature.

Key words: soil moisture; soil temperature; composite sensor; profile detection; performance analysis

0 Introduction

Soil moisture content is one of the key factors that affect the growth and yield of agricultural crops[1]. It is very important to obtain the vertical distribution of soil moisture content in real time for getting the distribution of crop root, variation of soil moisture and regular rules of crop water requirement[2-6]. Presently, the most common method is burying the pin type sensor in layered to acquire the vertical distribution of soil moisture content. However, this method has the disadvantages of inconvenient construction, damage to the local soil structure, and difficulty of replacing the unworkable sensor[7-12]. The layered non-contact measurement technology of soil moisture content and temperature has made great progress in both theory and practice abroad[13-14], such as EnviroSCAN sensor and Diviner 2000. But the domestic research in this area is still relatively defective. Principle of frequency domain reflection (FDR) is used in soil moisture content measuring in abroad products. Its sampling interval is 10 cm. In the measurement of soil moisture content, we must use the foreign manufacturers designed device to get data. Usually the price of these devices is very high. These products, at present, are not used widely. Thinking the above shortcomings and comparing the conventional soil moisture measuring methods[15-16], the feasibility of rapid detection of soil moisture content in multi-layered soil profile using Bobbi principle of dielectric theory[17-19] was analyzed. This paper designed a composite sensor based on SWR for soil profile to achieve measuring moisture and temperature of multilayer soil in real time.

Received date: 2015-05-19 Accepted date: 2015-06-29
Supported by National Natural Science Foundation of China (Grant No. 31171458)
Corresponding author: Zhao Yandong, Professor. E-mail: yandongzha@bjfu.edu.cn. Tel: +86-10-62336956.

1 Measurement principle and structure

1.1 Principle of moisture sensor

Using SWR method to measure soil moisture content was actually demonstrated via variation of characteristic impedance of the probe in the soil environment. Due to the mismatching of probe impedance and the characteristic impedance of the transmission lines, when high frequency electromagnetic waves transmitted along the line to the probe, a standing wave was produced on transmission line, which caused voltage amplitude change of transmission line ends. The principle of moisture sensor is shown in Fig. 1.

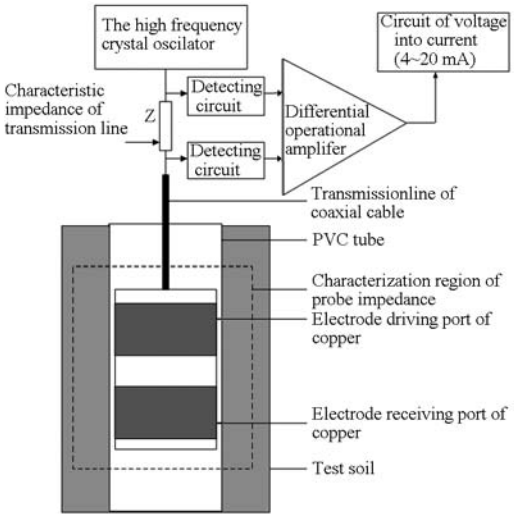

Fig. 1 Test environment and principle of soil moisture sensor

According to the theory of transmission line[20], the difference of transmission line ends ΔU is described as

$$\Delta U = 2A\rho = 2A\frac{Z_P - Z_I}{Z_P + Z_I} \tag{1}$$

Where ρ is the reflection of a transmission line index; A is the oscillation amplitude of high frequency oscillator; Z_P is the probe impedance; Z_I is the transmission line impedance.

If $Z_P = Z_I$, transmission line will not produce standing wave, so the voltage of transmission line ends are zero.

The impedance characteristics of the ring probe are related to the dielectric constant of the material filled in it. The capacitance value of ring probe is described as

$$C = g\varepsilon_r\varepsilon_0 \tag{2}$$

Where g is the constants related to shape size; ε_r is the dielectric constant of medium filled around ring probe; ε_0 is the dielectric constant in vacuum.

If taking the structure in Fig. 2 as the detection impedance model of the ring probe, then expression of its characterization capacitance is shown below

$$C_s = C_t + \frac{C_p C^*}{C_p + C^*} \tag{3}$$

Where C_s is the characterization capacitance of ring probe; C^* is the characterization capacitance of measured soil; C_t is the spurious capacitance generated by electric field.

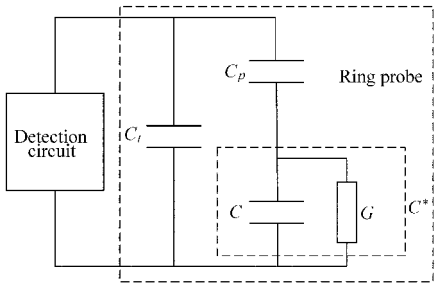

Fig. 2 Circuit model of ring probe detection impedance

It can be concluded from Eq. (2) that C^* and C_p can be calculated by $C^* = g_m\varepsilon_{r,m}\varepsilon_0$ and $C_p = g_p\varepsilon_{r,p}\varepsilon_0$.

Where the subscript m denotes the medium, and the subscript p denotes the plastic access tube; detection impedance Z_p and admittance Y of ring probe are expressed by

$$Y = \frac{1}{Z_P} = \mathrm{j}\omega C_s = \mathrm{j}\omega C_t + \frac{\mathrm{j}\omega C_p \mathrm{j}\omega C^*}{\mathrm{j}\omega C_p + \mathrm{j}\omega C^*} \tag{4}$$

Where ω is the test angular frequency of sensor.

In the detection process, the electrical conductivity of the soil will have an effect on the impedance of the probe[21].

$$\mathrm{j}\omega C^* = \mathrm{j}\omega C + G \tag{5}$$

Where G is the impedance produced by ionic conductivity of soil.

Due to the fixed-point measurement way that sensor adopts, it is considered that the disturbances from PVC pipe and spurious capacitance are fixed values. So sensor impedance is mainly decided by probe size and dielectric constant and working frequency.

In 1980, Topp et al.[22] obtained a single-valued mathematical relationship between soil dielectric constant and soil moisture content through the test method.

$$\theta = -5.3\times10^{-2} + 2.92\times10^{-2}\varepsilon - 5.5\times10^{-4}\varepsilon^2 + 4.3\times10^{-6}\varepsilon^3 \tag{6}$$

According to the above theories, soil moisture content can be measured by testing the change of sensor probe impedance.

1.2 Measurement principle of temperature sensor

The design of temperature measurement depended on the theory of platinum resistance, namely to reflect change of environmental temperature measured via the change of platinum resistance. Platinum resistance detection principle was shown in Fig. 3.

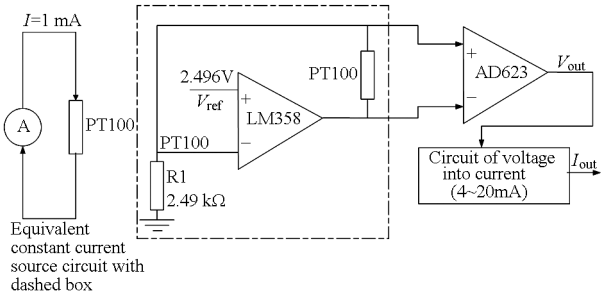

Fig. 3 Block diagram of soil temperature sensor

The 2.496 V reference voltage, namely V_{ref}, was generated by REF3025 chip, is exchanged to constant current source(1 mA) by operational amplifier.

When the current of constant current source flows through theplatinum resistance will produce pressure drop, then through differential operational amplifier AD623 the voltage signal of platinum resistance was picked up, and ultimately voltage signal output will be converted into 4 ~ 20 mA current signal.

$$V_{out} = \frac{V_{ref}}{R_1} R_{PT100} A_1 \quad (7)$$

$$I_{out} = V_{out} A_2 \quad (8)$$

Where V_{out} is output voltage values of sensor; V_{ref} is the 2.49 V reference voltage; R_1 is the 2.49 kΩ resistor; R_{PT100} is the resistance of PT100; A_1 is the magnification of differential operational amplifier AD623; A_2 is the factor of voltage-current conversion.

1.3 Configuration and structure of multilayer composite sensor for soil profile

Composite sensor for soil profile is made up by collecting main-board, moisture sensor, temperature sensor, connecting cable, PVC bracket and PVC sleeve, etc., as shown in Fig. 4. H is space of sensor probe (the shortest distance is 10 cm). The copper probe is layered muff-coupled on the PVC bracket, cylindrical in shape cylindrical shape. The copper probe interval conventional is 10 cm and it is adjustable. There are two moisture detection circuits internally and two copper electrodes embedded external using to receive/transmit electromagnetic signals. The number and location of moisture probe are determined according to actual needs (installing up to eight sensor probes). The temperature sensor board and moisture sensor circuit are connected by a connector, plugging in connecting cable. Sensor collecting main-board executed control and data collection to the sensors of each layer through connecting cable. In order to reduce the power of overall sensors and avoid the electromagnetic interference between the moisture sensors, time-sharing power supply mode of the sensor collecting main-board was taken for moisture and temperature sensor collecting board.

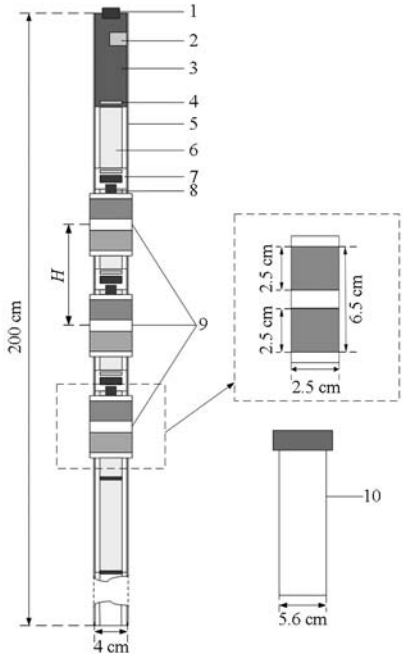

Fig. 4 Schematic of system configuration

1. Communication interface of power supply and RS-485 2. SD card storage module 3. Main-boardof sensor collecting part 4. Bottomed cable connector 5. PVC support frame 6. Connecting cables 7. Temperature sensor board 8. Main-board connector of moisture and temperature 9. Copper detection probe 10. PVC tube

Before using sensors, PVC pipe needed to be buried in the test point by specified tool. In the testing, position and number of moisture probe needed to be adjusted to meet the actual needs. Inserting the sensor PVC pipe, connecting to the power and data line and closing block button, online real-time measurement of soil moisture content and temperature can be implemented in different depths of soil.

1.4 Hardware circuit design of sensor

Measurement system diagram was shown in Fig. 5. The system mainly contained soil moisture detection unit, soil temperature detection unit and sensor collecting main-board. The sensor collecting main-board is made up by using STM32F103RBT6

microcontroller, SD card storage unit, current signal conversion unit, clock module, power conversion unit, power control unit and RS－485 interface unit.

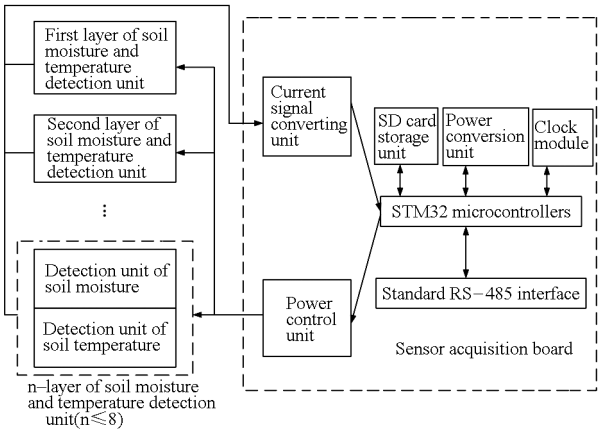

Fig. 5 Schematic diagram of measurement system

The system can set two kinds of working via the RS－485 interface mode, namely, independent working mode and sub-equipment working mode. Under the independent working mode, the sensor can carry out 12 V power supply to independently collect soil information. According to system setting time interval (default is 10 min), each layer of soil moisture and temperature information time-sharing was collected by power control unit when it is powered up. The collected information is stored to the SD card in the form of TXT. In the sub-equipment working mode, the controller of sensor ran the standard MODBUS sub-equipment communication protocol. The MODBUS master device with a RS－485 interface peripheral could control sensors to collect soil information in specified data frame.

2 Research on factors influencing soil moisture sensor impedance

2.1 Testing frequency, probe structure and dielectric properties of soil

It is important to research the impedance characteristics of moisture sensor probe in designing soil moisture sensor. The conventional moisture sensor probe is pin type structure, and its impedance characteristic mathematical model can be set up by the transmission line theory[25]. Compared to the pin type structure, the proposed impedance model of ring structure has some difficulties, such as, the probe shape is irregular and the boundary conditions of electromagnetic distribution is complex, it is difficult to find out analytic solution. With the help of a high frequency vector network analyzer, impedance characteristics of the ring electrode in four kinds of size were analyzed, eventually structure and working frequency of ring probe was determined. Taking the soil from the Beijing Forestry University experimental nursery (116°21′14″E,40°0′54″N) as samples, which were dried by oven (105 ℃, 24 h), we calculated the soil sample required moisture of soil different gradients. According to the calculated result to prepare soil, the 1.6 g/cm^3 bulk density soil was evenly loaded into seven PVC test buckets. The PVC test bucket's height were 50 cm, diameter was 40cm and in its central was fixed a PVC pipe with height of 50 cm and diameter of 5.6 cm. Seal and put it aside for 48 h to let soil moisture to migrate evenly. Take off the soil using ring knife and adopt drying method to measure the moisture contents of each test tube were 1.5%, 8%, 15%, 20%, 26%, 33% and 26%.

In order to test the effect of ring width, testing frequency and soil dielectric properties on probe impedance, four kinds of ring probe were selected to test. Their testing frequencies and widths respectively were 30, 100, 200, 300 MHz and 2.0, 2.5, 3.0, 3.5 cm, and their diameters were 2.5 cm and thickness were 0.09 cm. The tested soil sample was typical clay loam, its ingredient was 11% sand, 71% powder, and 18% sticky particles. The paper put forward using the three-dimensional simulation model to calculate the impedance characteristics of the capacitance probe, in the cases of the electrical conductivity of soil leaching liquor was very low, the effect on the change of overall probe impedance of real part was ignored[26], the electrical conductivity of the soil was only 0.20 mS/cm, the real part of the impedance characteristics was neglected. So paper only analyzed the imaginary part of the impedance of the ring probe. The vector network analyzer was used to measure the impedance of the probe. In the experiment, the single point was tested 10 times and the average value of the impedance was got to reduce the measurement error.

(1) Influence on impedance characteristics (Z_P) from testing frequency and width of the probe

In order to analyze the influence on probe impedance characteristics by change of testing frequency and size,

on the premise that the probe diameter and thickness were determined, we selected the copper ring electrode with width of 2.0, 2.5, 3.0, 2.5 cm to test the change of probe impedance with change of soil moisture content under different frequencies (30, 100, 200, 300 MHz), finally, obtained 112 sets data. Using the orthogonal method to carry out polynomial fitting between the data and the impedance of the probe, the fitting results was shown in Fig. 6 and Tab. 1.

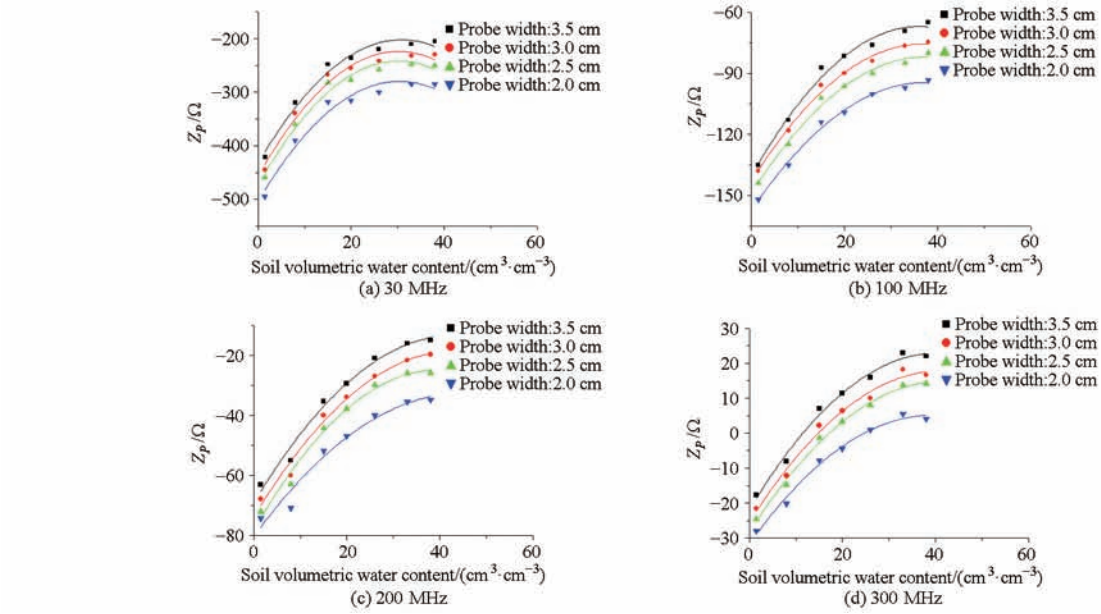

Fig. 6 Impedance curves of ring probe at different frequencies

According to Fig. 6 and Tab. 1, with a fixed structure of ring electrode, the impedance of the ring electrode was increased with the increasing frequency. However, with the fixed working frequency, the impedance was also positively correlated with the width of the copper ring electrode. When the working frequency was 100 MHz, the ring probe impedance was increased about 8 Ω with each 0.5 cm widened. The fitting curve showed that the determination coefficient (R^2) was more than 0.95. But when the frequency was 30 MHz, the fitting curve was not monotonous, which showed that the soil moisture content and the probe impedance were not single valued relationship, so soil moisture content could not be obtained directly by the probe impedance. When the frequency reached 30 MHz, the impedance of the ring probe was changed into the mutual conversion between the capacitive and inductive. This feature also leaded to the failure of direct get soil moisture by the probe impedance. Considering that in the low frequency, the soil was more easily influenced by soil electrical conductivity and the difficulties in realizing high frequency electronic circuit, 100 MHz was selected as sensor testing frequency.

(2) Influence on impedance of soil dielectric properties

In order to analyze the ring probe impedance characteristics affected by the soil dielectric property, taking clay loam in the Beijing City as the testing sample to prepare moisture gradient from air-dried soil to saturation moisture capacity (volumetric moisture content was about 40%). Sun et al.[28] presented a kind of determinations of soil dielectric constant using the principle of standing-wave ratio. In this paper, BD - Ⅲ - type soil moisture sensor that independently developed in Beijing Forestry University was used to calculate dielectric constant, which corresponding with soil moisture gradient. The contrast results of calculation and TOP equation were shown in Tab. 2. From Tab. 2, as we can see, there was a significant correlation between the experimental calculation and TOP equation results, it's proved that the experimental calculation results rightly illustrated out the dielectric properties of soil. The polynomial fitting was carried out between the calculated results and measured probe impedance using network analyzer. The fitting results were shown in Fig. 7. The probe width was 2.5 cm and working frequency was 100 MHz.

Tab. 1 Impedance fitting results of ring probes with different widths at different frequencies

Working frequency /MHz	Electrode width /cm	determination coefficient R^2	Polynomial fitting results
30	2.0	0.953 42	$y = -0.244x^2 + 14.826\ 23x - 504.985\ 43$
	2.5	0.969 26	$y = -0.256\ 08x^2 + 15.420\ 43x - 0.256\ 08$
	3.0	0.969 42	$y = -0.257\ 32x^2 + 15.518\ 02x - 457.740\ 57$
	3.5	0.971 13	$y = -0.243\ 64x^2 + 15.022\ 5x - 433.630\ 69$
100	2.0	0.990 59	$y = -0.045\ 24x^2 + 3.368\ 84x - 2.157\ 25$
	2.5	0.985 89	$y = -0.048\ 16x^2 + 3.595\ 9x - 149.066\ 85$
	3.0	0.990 34	$y = -0.049\ 78x^2 + 3.366\ 464x - 143.068\ 17$
	3.5	0.982 46	$y = -0.056\ 25x^2 + 4.064\ 1x - 140.411\ 9$
200	2.0	0.951 21	$y = -0.023\ 72x^2 + 2.127\ 04x - 80.338\ 76$
	2.5	0.980 44	$y = -0.034\ 11x^2 + 2.694\ 42x - 78.162\ 48$
	3.0	0.976 71	$y = -0.029\ 66x^2 + 2.558\ 68x - 73.793\ 34$
	3.5	0.977 53	$y = -0.030\ 17x^2 + 2.593\ 67x - 69.160\ 17$
300	2.0	0.986 56	$y = -0.023\ 8x^2 + 1.873\ 08x - 31.690\ 57$
	2.5	0.992 78	$y = -0.025\ 09x^2 + 2.079\ 08x - 28.247\ 49$
	3.0	0.981 03	$y = -0.025\ 26x^2 + 2.091\ 23x - 25.382\ 58$
	3.5	0.985 7	$y = -0.027\ 3x^2 + 2.211\ 9x - 21.845\ 83$

From the change of Fig. 7, it can be seen that the change of the port impedance of the probe and the change of dielectric constant were strong nonlinearity relationship. Dielectric constant in the range of 0 to 11, for example, the curve fell sharply, and then the curve changed obviously slowly. The soil dielectric constant was 25.1, which corresponding with saturated moisture content of tested soil. The volumetric moisture content of the dry soil was about 2%, corresponded dielectric constant was about 2.4. When the dielectric constant was between 2.4 and 25.1, the change of impedance was obvious. Therefore, the sensor probe could meet the detection needs of volumetric moisture content of the clayey soil.

Tab. 2 Soil dielectric constant

Medium	Dielectric constant of experiment calculation	Dielectric constant of TOP equation
Air	1.00	1.00
Volumetric soil moisture content of 2%	2.40	2.63
Volumetric soil moisture content of 9%	5.50	5.42
Volumetric soil moisture content of 16%	9.10	8.58
Volumetric soil moisture content of 22%	10.61	11.69
Volumetric soil moisture content of 27%	15.02	14.62
Volumetric soil moisture content of 30%	17.30	16.54
Volumetric soil moisture content of 35%	21.80	20.36
Volumetric soil moisture content of 39%	25.10	23.89
Water	81.00	81.00

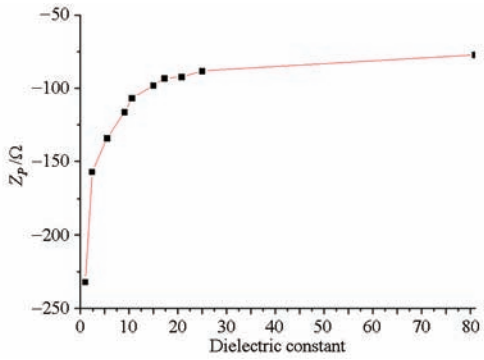

Fig. 7 Impedance curve with variation of dielectric constant of 2.5 cm ring probe at frequency of 100 MHz

2.2 Electric field distribution of ring probe

A model of ring probe was established by using electromagnetic field simulation software, namely HFSS. The solution frequency was 100 MHz. Excitation was lumped port. Probe diameter was 2.5 cm and widths, respectively, were 2.0, 2.5, 3.0, 2.5 cm. Dielectric constant of medium filled around the ring probe was setted as 21 (corresponding to the soil volumetric moisture content was 36%). The dielectric constant of installed PVC pipe and copper ring stent were 4. The medium in the PVC pipe was set to air and its dielectric constant was 1. The copper ring electrode was set in an ideal electric field boundary, and a cylinder with diameter of 12 cm and height of 13 cm were used as the radiation boundary condition.

From Fig. 8, some conclusions were obtained. Moisture content detection areas were mainly distributed among the probes, and the electric field was compacted and no separation phenomenon appeared. The ring probe with different widths mainly affected the longitudinal range and the horizontal range of the

electric field distribution in soil monitoring area. The electric field intensity was 104.9 V/m in light green areas of figure. The action scope of electric field strength which vertically reached to light green area of probe was increased with the increasing width of the copper ring, respectively, 9.5, 10.0, 10.5, 11.0 cm. Contrarily, the action scope of electric field strength which horizontally reached to light green area of probe reduced with the increased of the width of the copper ring, respectively, 10.5, 10.0, 9.5, 9.0 cm. From the above phenomenon it could be drawn that the four widths of the ring electrode were suitable to apply as the detection probe of sensor. In the application, the appropriate width of the ring electrode could be selected through the comprehensive consideration of the horizontal and vertical detection region. Considering that the conventional interval in the agricultural detection is 10 cm, the copper ring with the width of 2.5 cm was taken as the sensor electrode in this paper. From Fig. 8, we could see that the PVC pipe attenuated electric field intensity and the electric field intensity of inner copper ring was higher than that in the soil out of PVC pipe. Considering the influence of moisture testing board in copper ring on the electric field distribution, the metal shell shielding was designed on the moisture testing main-board.

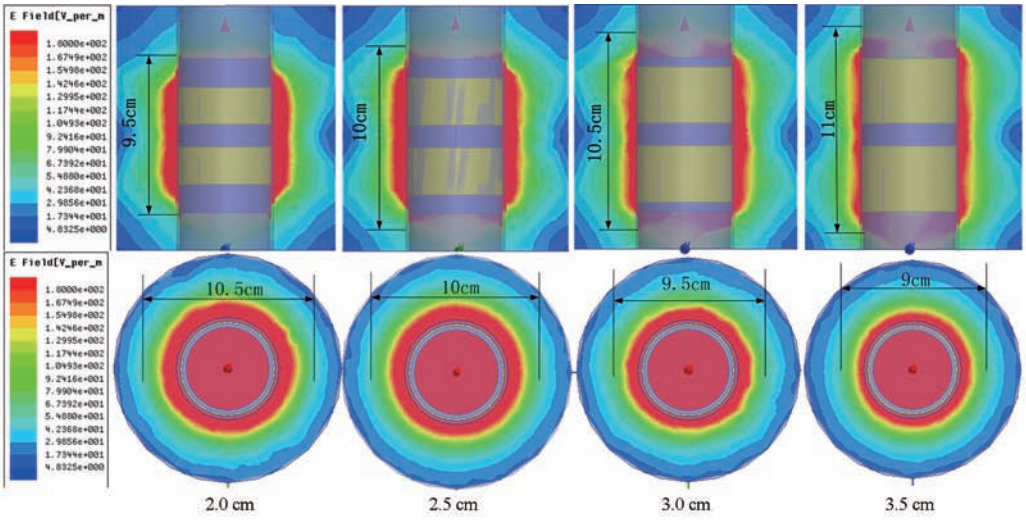

Fig. 8 Simulation of electrical field distribution of a ring probe

According to above analysis, the conclusion was proposed, namely the impedance of soil moisture sensor was related to its structure, measurement frequency and soil dielectric properties. But after the completion of the system structure design, the two parameters-structure and measurement frequency would no longer change, the impedance of the soil moisture sensor was only affected by the soil dielectric properties.

3 Performance test of sensor

3.1 Dynamic response performance test of sensor

(1) The dynamic response performance of the sensor, which was mainly manifested by the time required for complete response of the sensor when the moisture content changed in the sensor detection area. The experiment was divided into three steps. First of all, the probe of moisture sensor was loaded into PVC pipe, and it was put in PVC test barrels filled with water. An oscilloscope was used to measure the needed time just from powered sensor to its output stabilized was 1.28 ms. Then the sensor was raised from the PVC test pipe to the air. The time from sensor output to achieve stabilization was 500 ms. Finally, the sensor was put into PVC test pipe again, when sensor's outputs reached stabilized, the total time spent was 480 ms.

(2) The temperature detecting element adopted sheathed platinum resistance. The principle of the response time of the temperature measurement circuit was similar to that of the above. The dynamic response time of the test was 38, 720, 800 ms.

3.2 Calibration experiments and results of sensor

According to the measurement principle of temperature, the sensor output results were more susceptible to the effects of the accuracy of the components. So it needed to be calibrated before use. The SHP – 450 experimental boxes of Beijing Boyu

Baowei Experimental Equipment Co., Ltd. were adopted to calibrate the part of above 0℃. The boxes specific parameters constant temperature range was 0 to 60 ℃ and the accuracy was 0.1℃. Qingdao Haier group DW -40W255 type ultra cryopreservation box (-40 ~ 0℃) was used to calibrate the section of temperature below 0℃. The mercury thermometers with the precision of 0.1℃ were set in two devices as the reference temperature to improve the accuracy of sensor measurement results. The temperature ranged from -20℃ to 40℃, after heating and cooling, a mean value of each gradient, with 2℃ for gradient, was calculated and 29 sets of data were got. The temperature value of collector handled and mercury thermometer were fitted using the least square method. The output results were shown in Fig. 9.

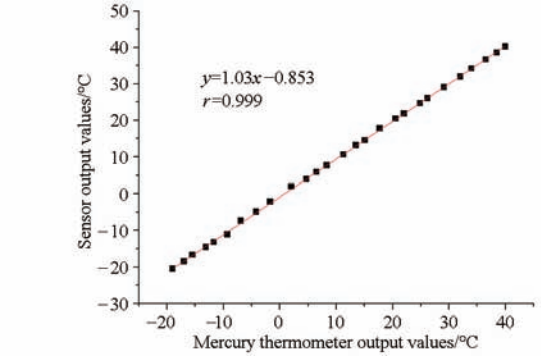

Fig. 9 Temperature sensor calibration curve

As can be seen from Fig. 9, the coefficient of determination r was 0.999, the output of the designed temperature sensor and mercury thermometers had a significant linear relationship with.

3.3 Calibration test and result of moisture sensor

(1) Experimental verification of sensor adaptability and sensitivity

The experiments were carried out in laboratory environment and the temperature was 25℃. Three kinds of different soil texture components, clay soil, sandy soil and clay loam, were used. The method of Section 2.1 was used to prepare these three kinds of test samples. Because of different saturation moisture capacities of soil, clay and clay loam in the 2% ~40% volumetric water content was set in ten gradients and sand in 2% ~ 30% was set in eight gradients. The data were voltage value that converted by collector. The data were carried polynomial fitting and the results were shown in Fig. 10.

Fig. 10 shows that there was a good correlation

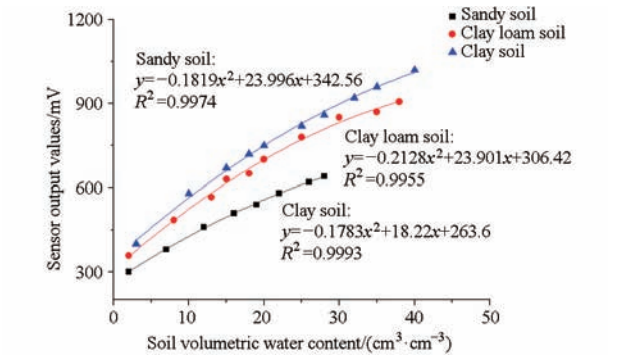

Fig. 10 Calibration curves of moisture sensor

between the output of sensor and soil volumetric water content in three kinds of soil,. Their determination coefficients, namely R^2, respectively were 0.997 4, 0.995 5 and 0.999 3. When moisture content increased by 10%, correspondingly, the voltage would change more than 100mV, which was voltage of the sensor output current after the conversion of the collector. This suggested that the sensor has good sensitivity.

(2) Calibration experiment and compensation mode on the influence of temperature

Temperature had a great effect on both soil dielectric properties and measurement accuracy. It was important to compensate measurement accuracy of the composite sensor using effective ways. The three kinds of different soil texture components, clay soil, sandy soil and clay loam, were used to conduct an experiment. The three kinds of soil were arranged into the soil samples in four kinds of different volumetric moisture content taking the method of Section 2.1. The volumetric moisture content of the clay loam were: 8%, 15%, 26%, 37% and clay soil volumetric moisture content were 10%, 18%, 24%, 39% and sandy soil volumetric moisture content were 5%, 10%, 16%, 25%. In turn, the soils were loaded into four PVC test buckets with height of 20 cm and diameter of 20 cm (its central fixed a PVC pipe with 20 cm height and 5.6 cm diameter). The plastic wrap was sealed and put aside for 48 h to let soil moisture migrate evenly. The composite sensor probe developed in this paper was placed in the PVC pipe filled with soil sample, and then sealed with heat insulation cotton to prevent heat Incoming from the PVC pipe. The PVC test buckets were placed in the drying box. When the temperature change rang of the drying box was 25 ~ 50℃ and the change of gradient was 5℃, the soil temperature was detected by using the temperature

detection unit of the composite sensor probe. When the detected temperature was consistent with the temperature set by the drying box, the output voltage of the moisture detection unit of the composite probe was recorded. According to the above method, the soil samples of the other two samples were measured, and the 72 sets of data were produced. To take off the soil using ring knife after test, the moisture content of each soil samples was measured by using the drying method. Experiment results were shown in Fig. 11 and Tab. 3.

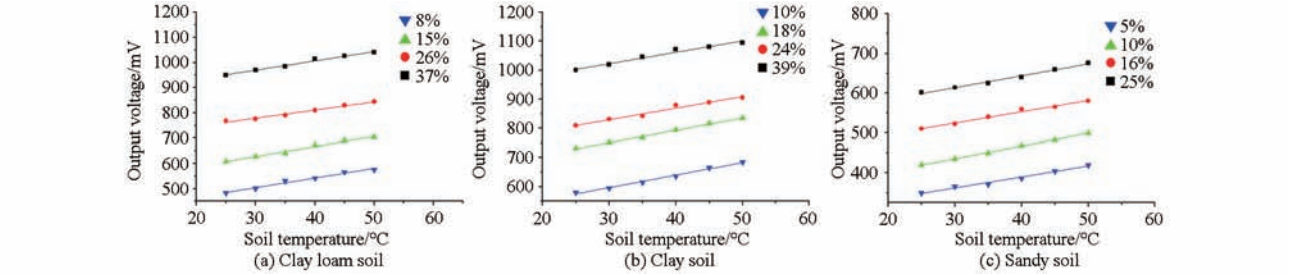

Fig. 11 Relationship between sensor output and soil temperature

Tab. 3 Fitting results of determination coefficient

Soil type	Volatile water content/%	R^2	Linear relevant fitting result
Clay loam soil	8	0.982 3	$y = 3.84x + 388.67$
	15	0.988 5	$y = 3.982\,9x + 507.81$
	26	0.987 1	$y = 3.24x + 681.33$
	37	0.989 1	$y = 3.691\,4x + 858.9$
Clay soil	10	0.991 7	$y = 4.32x + 467.33$
	18	0.996 8	$y = 4.205\,7x + 624.95$
	24	0.977 2	$y = 3.977\,1x + 710.19$
	39	0.976 2	$y = 3.914\,3x + 905.38$
Sandy soil	5	0.980 8	$y = 2.754\,3x + 279.71$
	10	0.998 3	$y = 3.182\,9x + 340.14$
	16	0.985 8	$y = 2.845\,7x + 439.29$
	25	0.988 5	$y = 2.988\,6x + 524.1$

It's known that from Fig. 11, output voltage of moisture detection unit in composite sensor in measurement of the three kinds of soil and the soil temperature of the composite sensor in the increasing of soil temperature were positively correlated. The main reason was that the increasing temperature would increase the degree of polarization of the molecules and the movement of the moisture molecules in the soil, resulting in the increase of the dielectric constant of the soil. In addition, the change of environmental temperature also affected the output characteristics of electronic components in the sensor. These results showed that the change of soil temperature had a certain effect on the output of the water detection unit in composite sensor. In order to eliminate the influence of environmental temperature on sensor output, the data of three kinds of soil were analyzed by SPSS software using linear regression method. Based on the experiment soil, the relationship between temperature, soil moisture content and output voltage of the sensor was obtained according to the experiment results. The model was shown in Tab. 4.

Tab. 4 Linear regression model of three kinds of soil

Soil type	F test p value	Adjustment value ($p = 0.05$)	Model of linear regression
Clay loam soil	0	0.982 3	$V_{out} = 1\,568.832\theta_v + 3.689T + 271.88$
Clay soil	0	0.991 7	$V_{out} = 1\,112.562\theta_v + 4.104T + 448.889$
Sandy soil	0	0.980 8	$V_{out} = 1\,263.438\theta_v + 2.943T + 218.928$

From Tab. 4 it can be seen that the F values of measured soil were 0. When the significance level was 0.5, adjustment R^2 was more than 0.98. It suggested that two regression models well reflected the relationship between the output voltage of the sensor and the moisture content and temperature in the soil.

3.4 Analysis of anti-interference in layer-to-layer of composite sensor

In order to eliminate the influence on the sensor output of the interferences between the sensor probes, this paper used the time-sharing power mode, that means, the power mode was controlled by using sensor collecting main-board for realizing that at the same time only one sensor was working.

The test object was a soil profile composite sensor withtwo detection probes. The soil samples, of which volumetric water content was 28%, was prepared by using the method and container. The sensor was inserted into the test soil. The lower edge of the upper probe was adjusted to approximately 1 ~ 20 cm above

the top edge of the under probe. The output value of the two sensor probes were measured with 1cm as the step size. The output results were shown in Fig. 12.

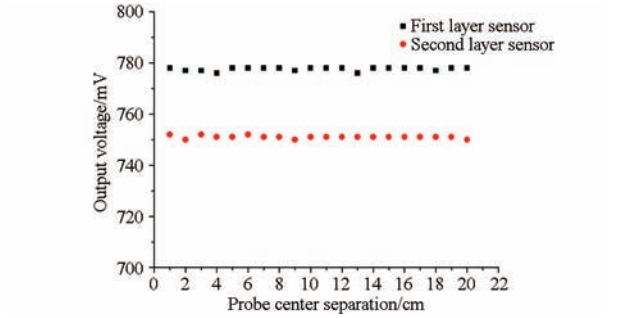

Fig. 12 Relationship between sensor output voltage and probe spacing

Fig. 12 showed that the output values of the two sensor probes were not changed with the change of distance. Because the time-sharing method was adopted on the powered sensor probe, the spacing between sensor probes had no effect on the sensor output.

4 Dynamic test in field

In order to verify the reliability and adaptability of the soil composite sensor, experiments were conducted in Xiaotangshan National Precision Agriculture Demonstration Base, Changping District, Beijing City, in March, 2014. The experiment field was a lysimeter with volume of 1 m × 1 m × 2.5 m. The soil was clay loam soil, and the experiment field was planted with winter wheat. The PVC test pipe was installed in the lysimeter. Before the test, the sample soil was collected and calibrated using method in Section 3.2. And then the specific installation tool was punch and embedded into the PVC test pipe with length of 1 m, as far as possible to avoid destruction of soil samples to reduce the disturbance to the minimum. The installation depth of the composite sensor probe was 30, 60, 90 cm. The whole test system used solar power to drive. The interval of data collecting was 30 min. Fig. 13 showed the test environment.

The detection data from the April 15 – 22, 2014 were shown in Fig. 14. As you can see by the figure, the temperature and volumetric moisture content of soil presented continuous cycle variation over time. In the shallow layer soil (30 cm), the temperature and volumetric moisture content were affected by the change of day and night. At the same time, because

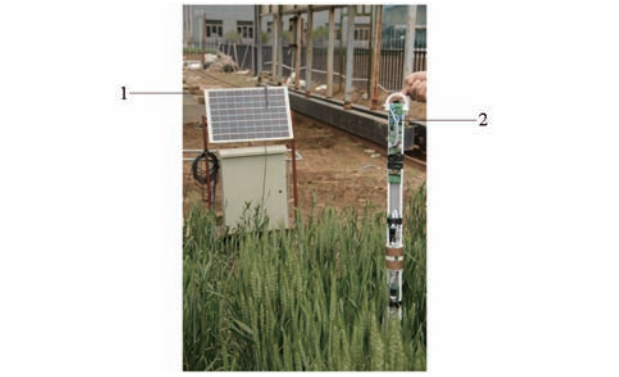

Fig. 13 Field test site

1. Solar power system 2. Soil planning surface composite sensor

the wheat were at heading stage, and the water needed was bigger, that further leaded to the change of soil volumetric moisture content more strongly in area of wheat root (30 cm). As the water in the root zone was lacking, the soil moisture would be added to the root zone due to the capillary phenomenon and the absorption of the crop root, so the soil volumetric moisture content of 60 cm was lower than that of 30 cm.

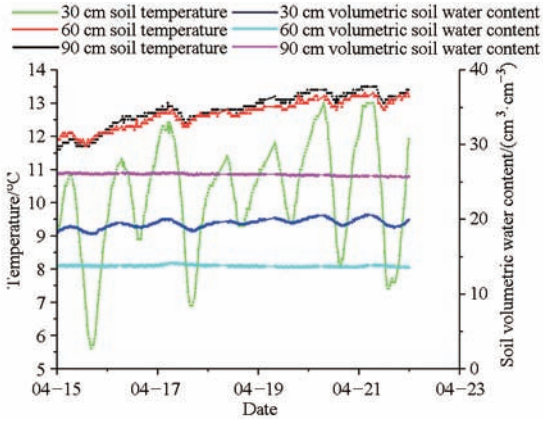

Fig. 14 Dynamic change curves of soil moisture and temperature at different depths

As the test pipe was installed in the lysimeter, there was no supplement of the underground water source. The soil volumetric moisture content of 90 cm was lower than that in the field saturation moisture capacity, it was not enough to add water to 60 cm. So the soil volumetric moisture content of 60 cm was lower than that of 90 cm.

The effect of plant root zone on the output of soil composite sensor was not considered in design. However, in practical application, many plant rootswere distributed in soil, which would affect the output of the sensor. The sensor can be corrected by the method of establishing regression model of the root

zone density and the corresponding sensor output. This also needs to be improved in the design.

5 Conclusions

(1) A soil profile composite sensor was proposed to realize the real-time detection of temperature and soil moisture content of multi-layer soil profile. It has great significance for the detection of soil volumetric moisture content and temperature in plant root zone. And it is also very important to study the migration of soil moisture and temperature.

(2) In depth studied of the sensor testing frequency and probe structure. With the aid of network vector analyzer, the impedance characteristics of the four dimensions of the ring probes at different gradient moistures were analyzed. The electric field distribution of the ring electrode was simulated by the HFSS. Finally, parameters of the sensor were determined: the diameter was 5 cm, the width was 2.5 cm, the thickness of the copper ring structure was 0.09 cm and the test frequency was 100 MHz.

(3) From laboratory calibration and experiment results, characteristics of proposed sensor can be drawn as: high accuracy, adaptability, sensitivity and eminent dynamic response performance. In moisture detection part of the composite sensor in three different textures soil experiments showed that the proposed sensor has a high adaptability, the determination coefficients of the polynomial fitting of clay, clay loam and sandy soil were 0.997 4, 0.995 5 and 0.999 3. In temperature detection part, the output of the composite sensor temperature detection unit and the measured value were linear fitted and the correlation reached 0.999.

(4) The effects of temperature and volumetric moisture content of soil on the output of the sensor were analyzed by means of experiments. The models of the sensor at different temperatures were established using statistical regression method.

(5) Continuous experiments in field showed that the soil profile composite sensor can correctly reflect the information of temperature and moisture in soil profile and it has high reliability.

References

[1] Li Lianjun, Sun Yurui, Lin Jianhui. A wireless-sensor for soil water content powered by solar energy [J]. Journal of Jiangsu University: Natural Science Edition, 2009, 30(6): 541 - 544. (in Chinese)

[2] Kang S, Zhang J. Controlled alternate partial root-zone irrigation: its physiological consequences and impact on water use efficiency[J]. Journal of Experimental Botany, 2004, 55(407): 2437 - 2446.

[3] Hutton R J, Loveys B R. A partial root zone drying irrigation strategy for citrus-effects on water useefficiency and fruit characteristics [J]. Agricultural Water Management, 2011, 98(10):1485 - 1496.

[4] Hedley C B, Yule I J. A method for spatial prediction of daily soil water status for precise irrigation scheduling [J]. Agricultural Water Management, 2009, 96(12): 1737 - 1745.

[5] Thompson R B, Gallardo M, Valdez L C, et al. Using plant water status to define threshold values for irrigation management of vegetable crops using soil moisture sensors [J]. Agricultural Water Management, 2007, 88(1/2/3):147 - 158.

[6] Gao Xiaodong, Wu Pute, Zhao Xining, et al. Estimating the spatial means and variability of root-zone soil moisture in gullies using measurements from nearby uplands[J]. Journal of Hydrology, 2013, 476(1): 28 - 41.

[7] Sheng W, Sun Y, Lammers P S, et al. Observing soil water dynamics under two field conditions by a novel sensor system [J]. Journal of Hydrology, 2011, 409(1/2):555 - 560.

[8] Li Xiaodong, Wu Yongfeng, Li Guanglin, et al. Development of wireless soil moisture sensor based on solar energy[J]. Transactions of the Chinese Society of Agricultural Engineering, 2010, 26(11): 13 - 18. (in Chinese)

[9] Zhao Yandong, Ma Yangfei, Wang Yongzhi. Green land precision irrigation control system and analysis of optimal irrigation amount[J]. Translations of the Chinese Society for Agricultural Machinery, 2012, 43(3):46 - 50. (in Chinese)

[10] Steven R, Robert C, Joaquin J, et al. Soil water sensing for water balance, ET and WUE [J]. Agricultural Water Management, 2012, 104(2): 1 - 9.

[11] Zhao Yandong, Wang Yiming. Intelligent system of measuring the spatial distributions of Soil moisture[J]. Transactions of the Chinese Society for Agricultural Machinery, 2005, 36(2): 76 - 78. (in Chinese)

[12] Peng Zengyu, Zhao Yandong. A monitoring system of real-time soil water content based on μC/OS-Ⅱ operating system [J]. Journal of Beijing Forestry University, 2010, 32(6): 114 - 119. (in Chinese)

[13] Dean T J, Bell J P, Baty AJB. Soil moisture measurement byan improved capacitance technique: Part

I Sensor design and performance [J]. Journal of Hydrology, 1987 93: 67 - 78.

[14] Paltineanu I C, Starr J L. Real-time soil water dynamics using multi sensor capacitance probes: laboratory calibration[J]. Soil Science Society of America Journal, 1997, 61: 1576 - 1585.

[15] Zhang Xueli, Hu Zhenqi, Chu Shili. Methods for measuring soil water content: a review[J]. Chinese Journal of Soil Science, 2005, 36(1): 118 - 121. (in Chinese)

[16] Cai Kun, Yue Xuejun, Hong Tiansheng, et al. Design of soil water content sensor based on phase-frequency characteristics of RC networks[J]. Transactions of the Chinese Society of Agricultural Engineering, 2013, 29(7): 36 - 43. (in Chinese)

[17] Ortuani B, Benedetto A, Giudici M, et al. A non-invasive approach to monitor variability of soil water content with electromagnetic methods [J]. Procedia Environmental Sciences, 2013, 7(19): 446 - 455.

[18] Cardenas-Lailhacar B, Dukes M D. Precision of soil moisture sensor irrigation controllers under field conditions[J]. Agricultural Water Management, 2010, 97(5): 666 - 672.

[19] Zhao Yandong, Wang Yiming. Study on the measurement of soil water content based on the principle of standing-wave ratio[J]. Transactions of the Chinese Society for Agricultural Machinery, 2002, 4(33): 109 - 111, 121. (in Chinese)

[20] Fan Shoukang, Lu Chunlan, Li Pinghui. Microwave technology and microwave circuit[M]. Beijing: China Machinery Industry Press, 2003. (in Chinese)

[21] Hilhorst M A. Dielectric characterization of soil[D]. Wageningen Agric. Univ., Wageningen, The Netherlands, 1998.

[22] Topp G C, Davis J L, Annan A P. Electromagnetic determination of soil water content: measurements in coaxial transmission lines [J]. Water Recourse Research, 1980, 16(3): 574 - 582.

[23] He Shusen, Huang Muli. The application of micro-computer in the testing of field water depth [J]. Transactions of the Chinese Society for Agricultural Machinery, 1998, 29(1): 130 - 135. (in Chinese)

[24] Zhang Daohui, Zhao Hongjun, Zhou Guangfang, et al. Drift of the temperature-controlled instrument for the farm products storage[J]. Transactions of the Chinese Society for Agricultural Machinery, 2010, 41(6): 108 - 112. (in Chinese)

[25] Zhao Yandong, Nie Mingjun. Optimal analysis for determining the dual-pin length of soil moisture probe [J]. Transactions of the Chinese Society for Agricultural Machinery, 2011, 42(11): 39 - 43. (in Chinese)

[26] Ma Daokun, Sun Yurui, Wang Maohua, et al. Three-dimensional numerical modeling of a four-pin probe for soil water content [J]. Australian Journal of Soil Research, 2006, 44: 183 - 189.

[27] Zhao Yandong. Study on fast-measurement of soil water content and application technology [D]. China Agricultural University, 2002. (in Chinese)

[28] Sun Yurui, Wang Baohua, Zhao Yandong. A kind of determinations of soil dielectric constant using the principle of standing-wave ratio[J]. Transactions of the Chinese Society of Agricultural Engineering, 1999, 15(2): 43 - 47. (in Chinese)

[29] Guo Wenchuan, Zhang Peng, Song Kexin, et al. Dielectric properties of Lou soil and moisture content detection affected by frequency and temperature[J]. Journal of Drainage and Irrigation Machinery Engineering, 2013, 31(8): 713 - 718. (in Chinese)

doi:10.6041/j.issn.1000-1298.2016.01.015

多层土壤剖面复合传感器设计与性能分析

高志涛[1,2]　刘卫平[1,2]　赵燕东[1,2]　张超一[1,2]

(1.北京林业大学工学院,北京 100083;2.北京林业大学城乡生态环境北京实验室,北京 100083)

摘要:针对土壤剖面温度与水分检测存在传感器安装困难、对本地土壤扰动比较大等问题,设计了一种基于驻波比土壤水分测量原理与基于铂电阻测温原理的多层土壤剖面复合传感器。借助矢量网络分析仪与 HFSS 电磁场仿真软件对传感器电极的阻抗特性与电场分布状况进行了分析,确定了铜质检测探头结构为:直径 5 cm、宽度 2.5 cm、厚度 0.09 cm,测试电路激励频率为 100 MHz。以 3 种不同质地土壤作为测试样本,对土壤水分与温度检测单元的输出与对应的测量值分别进行了多项式拟合与线性拟合,相关性均达到 0.99 以上,系统稳态及动态性能均满足土壤剖面温度与水分的检测要求。通过试验分析了土壤温度与体积含水率对传感器输出的影响,利用统计回归方法建立了传感器在不同温度时的修正模型。在北京市小汤山野外环境下,将传感器工作于埋入土壤的 PVC 管体中,同时获取 3 层土壤温度与水分剖面信息,数据可靠,性能稳定,为实时获取多层土壤墒情及土壤温度提供了一种高效方法。

关键词:土壤水分;土壤温度;复合传感器;剖面测量;性能分析

中图分类号:S237　　**文献标识码**:A　　**文章编号**:1000-1298(2016)01-0108-10

Design and Performance Analysis of Composite Sensor for Multilayer Soil Profile

Gao Zhitao[1,2]　Liu Weiping[1,2]　Zhao Yandong[1,2]　Zhang Chaoyi[1,2]

(1. *School of Technology*, *Beijing Forestry University*, *Beijing* 100083, *China*

2. *Beijing Laboratory of Urban and Rural Ecological Environment*, *Beijing Forestry University*, *Beijing* 100083, *China*)

Abstract: Considering the many difficulties of installing the sensor for the soil temperature and moisture measurement, such as miserable installation of the sensor and relatively large disturbance to the local soil, this paper designed a composite sensor for multilayer soil profile in accordance with the principles of soil moisture measurement and temperature measurement based on SWR and platinum resistance. A vector network analyzer and HFSS electromagnetic simulation software were used to analyze impedance characteristic and electric field distribution of the sensor electrode. According to the analysis result, the structure of copper detection probe was designed. The diameter of the probe is 5 cm, the width is 2.5 cm, the thickness is 0.09 cm and the excitation frequency of test circuit is 100 MHz. Three types of soil were choosen as experimental samples. The polynomial fitting and linear fitting were conducted on the output values of sensor detection unit. The results correlation reached more than 0.99. The static and dynamic performance of the system met the detection requirements of temperature and moisture of soil profile. Experiments was carried out in Xiaotangshan District, Beijing City, and then effect of temperature and volumetric moisture content of soil on sensor outputs were analyzed and correction models were established by using the statistical regression method at different temperatures. The sensor working in the PVC pipe buried in the soil could obtain the information of temperature and moisture of the three

收稿日期:2015-05-19　修回日期:2015-06-29

基金项目:国家自然科学基金项目(31171458)、北京市教育委员会科学研究与研究生培养共建项目(BLCXY201519)和北京市共建项目

作者简介:高志涛(1989—),男,博士生,主要从事生态信息智能检测与控制研究,E-mail:e228319@163.com

通信作者:赵燕东(1965—),女,教授,博士生导师,主要从事生态信息智能检测与控制研究,E-mail:yandongzh@bjfu.edu.cn

layers, and its performance was stable and the data was reliable. This study provides a highly efficient method for obtaining the real-time information of multilayer soil moisture and temperature.

Key words: soil moisture; soil temperature; composite sensor; profile detection; performance analysis

引言

土壤含水率是影响农田作物生长与产量的关键因素之一[1]。实时了解土壤含水率的垂直分布对于了解作物根系分布、土壤墒情变化、作物的需水规律具有十分重要的意义[2-6]。目前，通常是采用插针式传感器分层埋设，但这种方法存在施工不便、破坏本地土壤结构、传感器损坏更换困难等缺点[7-12]。对于土壤含水率与温度分层非接触测量技术，国外已经在理论和实际产品中取得了很大进展[13-14]，如 Sentek 公司的 EnviroSCAN 土壤水分扩线系统与 Diviner2000 土壤水分廓线仪。但国内在这一方面的研究还比较欠缺。

国外此类型产品通常采用频域反射(FDR)测量原理，采样间隔为 10 cm。使用国外设备进行数据采集，价格昂贵，目前主要用于科学研究上。针对上述缺点，在常规土壤水分测量方法[15-16]基础上，探讨采用介电理论中的驻波比原理对多层剖面土壤含水率快速测定的可行性[17-19]，设计一款基于驻波比原理，能够实时测量多层土壤含水率与温度的土壤剖面复合传感器。

1　测量原理与结构

1.1　水分传感器的测量原理

利用驻波比法测量土壤含水率实际上反映的是土壤环境中探头的特性阻抗变化。当高频电磁波沿传输线传送到探头时，由于探头阻抗与传输线的特性阻抗的不匹配，会在传输线上产生驻波，从而引起传输线两端电压幅值的变化。传感器测量原理如图 1 所示。

根据传输线理论[20]

$$\Delta U = 2A\rho = 2A\frac{Z_P - Z_I}{Z_P + Z_I} \tag{1}$$

式中　ΔU——传输线两端电势差

A——高频振荡器的振荡幅值

Z_P——探头阻抗

Z_I——传输线阻抗

ρ——传输线的反射指数

当 $Z_P = Z_I$ 时，传输线上不会产生驻波，传输线两端电压为零。

环形探头的阻抗特性与其内部的填充物质的介电常数有关，即

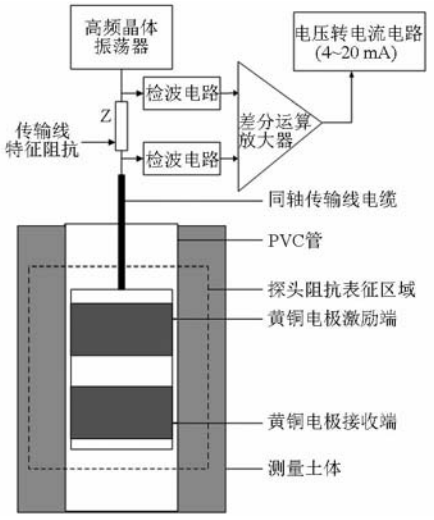

图 1　传感器测试环境与原理图

Fig. 1　Test environment and principle of soil moisture sensor

$$C = g\varepsilon_r\varepsilon_0 \tag{2}$$

式中　C——环形探头电容

g——与形状尺寸有关的常数

ε_r——探头周围填充介质的介电常数

ε_0——真空中的介电常数

假设环形探头的检测阻抗模型如图 2 所示，其探头表征电容的表达式为

$$C_s = C_t + \frac{C_p C^*}{C_p + C^*} \tag{3}$$

其中　$C^* = g_m\varepsilon_{r,m}\varepsilon_0 \qquad C_p = g_p\varepsilon_{r,p}\varepsilon_0$

式中　C_s——环形探头的表征电容

C^*——测量土壤的表征电容

C_p——传感器探头周围的 PVC 安装管所表征的电容

C_t——电场所产生的杂散电容

g_m——与土壤相关的常数

g_p——与 PVC 管体相关的常数

$\varepsilon_{r,m}$——探头周围填充土壤的响应介电常数

$\varepsilon_{r,p}$——探头周围 PVC 管的响应介电常数

环形探头的检测阻抗值 Z_P 与导纳 Y 可表示为

$$Y = \frac{1}{Z_P} = \mathrm{j}\omega C_s = \mathrm{j}\omega C_t + \frac{\mathrm{j}\omega C_p \mathrm{j}\omega C^*}{\mathrm{j}\omega C_p + \mathrm{j}\omega C^*} \tag{4}$$

式中　ω——传感器的测试角频率

检测过程中土壤离子电导率会对探头的阻抗特性产生影响[21]，有

$$\mathrm{j}\omega C^* = \mathrm{j}\omega C + G \tag{5}$$

式中　G——土壤中离子电导率的影响产生的阻抗

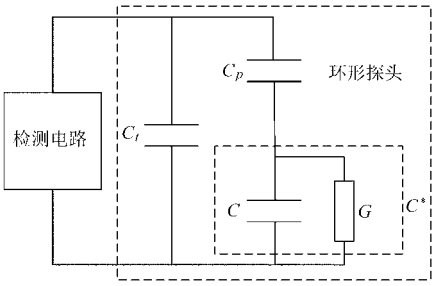

图 2 环形探头检测阻抗电路模型

Fig. 2 Circuit model of ring probe detection impedance

由于传感器采用定点测量,可以认为 PVC 管与电路杂散电容对其的影响是固定值。所以其阻抗主要由传感器探头尺寸、探头检测土壤的介电常数与工作频率决定。

1980 年 Topp 等[22]通过试验方法得出了土壤介电常数 ε 与土壤含水率 θ 之间存在单值数学关系

$$\theta = -5.3\times10^{-2} + 2.92\times10^{-2}\varepsilon - 5.5\times10^{-4}\varepsilon^2 + 4.3\times10^{-6}\varepsilon^3 \quad (6)$$

基于上述理论可以通过测量传感器探头阻抗的变化来测量土壤含水率。

1.2 温度传感器的测量原理

温度采用铂电阻测温原理,通过铂电阻阻值的变化检测环境温度的变化[23-24]。铂电阻阻值检测原理如图 3 所示。

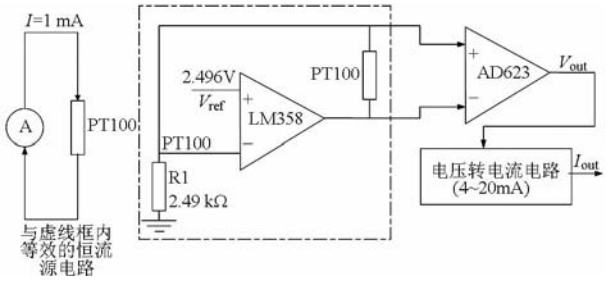

图 3 温度测量原理图

Fig. 3 Block diagram of soil temperature sensor

芯片 REF3025 产生 2.496 V 基准电压 V_{ref},通过运放 LM358 转换成恒流源(1 mA),电流流经铂电阻(PT100)产生压降,再由差分运算放大器 AD623 拾取铂电阻上的电压信号,最终通过电压电流转换芯片 AD694 将输出的电压信号转换成 4 ~ 20 mA 的电流信号。

$$V_{out} = \frac{V_{ref}}{R_1} R_{PT100} A_1 \quad (7)$$

$$I_{out} = V_{out} A_2 \quad (8)$$

式中 V_{out}——传感器输出的电压

V_{ref}——参考电压,取 2.49 V

R_1——理想电阻 R1 阻值,取 2.49 kΩ

R_{PT100}——PT100 铂电阻的阻值

A_1——差分运放 AD623 的放大倍数

A_2——压电流转换系数

1.3 土壤剖面复合传感器组成及结构

本文设计的土壤剖面复合传感器由采集主板、水分传感器、温度传感器、连接线缆、PVC 支架、PVC 套筒等组成,如图 4 所示。图中 H 为传感器探头间距(最短距离为 10 cm),铜制检测探头分层(常规间隔 10 cm,可调整)套接在 PVC 支架上,呈圆柱形结构,内含水分检测电路,外部嵌有 2 个黄铜电极用于接收发送电磁波。水分探头可根据实际需要确定个数和位置(最多可安装 8 个传感器探头),温度传感器主板与水分传感器电路通过连接件连接,插接在连接线缆上。传感器采集主板通过连接线缆对每层的传感器进行控制与数据采集。为了降低传感器整体功率,避免水分传感器间的电磁干扰,传感器采集主板对水分传感器与温度采集板采用分时供电的方式。

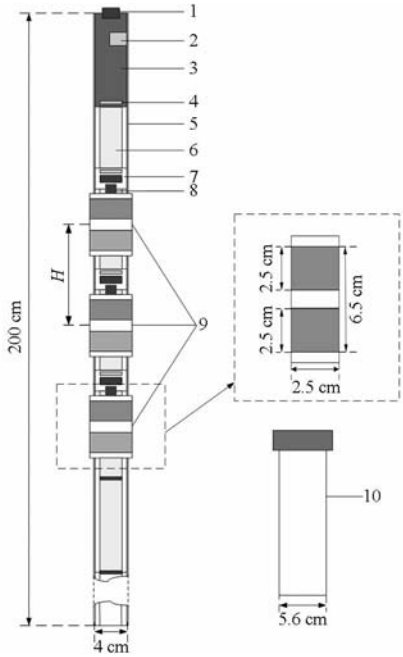

图 4 系统组成及结构示意图

Fig. 4 Schematic of system configuration

1. 电源与 RS-485 通信接口 2. SD 卡存储模块 3. 传感器采集主板 4. 底部排线连接件 5. PVC 支架 6. 连接线缆 7. 温度传感器主板 8. 水分主板与温度主板连接件 9. 铜制检测探头 10. PVC 套筒

在使用传感器之前,需要使用指定的工具将 PVC 管埋设在测试点。测试时,根据实际测量需要,调整水分探头的位置与个数,将传感器插入 PVC 管体中,接上电源与数据线,扣紧密封盖,即可实施不同深度土壤含水率与温度的在线实时测量。

1.4 传感器的硬件电路设计

系统原理框图如图 5 所示,主要包括土壤含水率检测单元、土壤温度检测单元与传感器采集主板。采集主板包括微控制器 STM32F103RBT6、SD 卡存

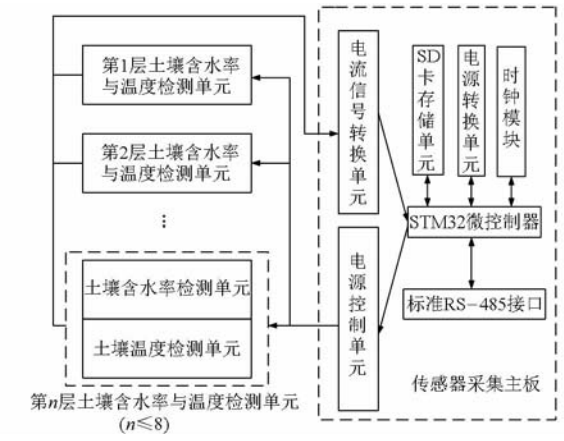

图 5　系统原理框图

Fig. 5　Schematic diagram of measurement system

储单元、电流信号转换单元、时钟模块、电源转换单元、电源控制单元、RS－485 接口单元。

该系统可以通过 RS－485 接口设置 2 种工作模式，分别为独立工作模式与子设备工作模式。在独立工作模式下，传感器只需直流 12 V 供电即可独立进行土壤信息采集工作，采集主板依据系统设定的采集时间间隔（默认 10 min），通过电源控制单元对土壤每层的温度与水分信息分时上电采集，采集的信息以 TXT 文本的形式存储至 SD 卡；在子设备工作模式下，传感器控制器运行标准的 MODBUS 子设备通信协议，外部带有 RS－485 采集接口的 MODBUS 主设备均可以按照指定数据帧控制传感器对土壤信息进行采集。

2　土壤水分传感器阻抗影响因子研究

2.1　测试频率、探头宽度与土壤的介电常数对传感器阻抗的影响

水分传感器探头阻抗特性的研究是设计土壤水分传感器的重要环节，常规水分传感器的探头多为针式结构，其阻抗特性的数学模型可以通过传输线理论建立[25]。相比于针式结构，环式结构阻抗模型研究存在探头形状不规则与电磁分布边界条件复杂等困难，很难求出解析解。本文借助一台高频网络矢量分析仪（NA7300 型，天津德力电子仪器公司，阻抗 50 Ω，扫描频率 0.3 ~ 3 000 MHz，频率分辨率10 Hz）对 4 种尺寸环形电极的阻抗特性进行了分析，最终确定了环形探头宽度与工作频率。测试土壤样本取自北京林业大学试验苗圃（116°21′14″E，40°0′54″N），通过烘箱（105℃，24 h）进行干燥。计算土壤不同梯度含水率的土壤样本所需水分，配比后土壤容重按 1.6 g/cm^3 均匀装入高 50 cm、直径 40 cm，中心固定有高 50 cm、直径 5.6 cm 的 PVC 管的 7 个 PVC 测试桶中。密封静置 48 h，使土壤中的水分运移均衡。利用环刀取土，采用烘干法测得每个测试筒的土壤含水率分别为 1.5%、8%、15%、20%、26%、33% 与 38%。

为了检验环形探头宽度、测试频率与土壤介电常数对探头阻抗的影响，选取直径为 2.5 cm、厚度为 0.09 cm，宽度分别为 2.0、2.5、3.0、3.5 cm 的 4 种环形探头，测试频率分别选取 30、100、200、300 MHz。测试土样为典型粘壤土，其成分构成为：砂粒 11%、粉粒 71%、黏粒 18%（以上均为质量分数）。文献[26]中提出，在土壤的浸出液电导率很低的情况下，可以忽略阻抗实部对探针整体阻抗变化的影响。本文所测土壤的浸出液电导率仅为 0.20 mS/cm，所以在试验中忽略了阻抗特性的实部，只对环形探头阻抗的虚部进行分析。

采用矢量网络分析仪对探头的阻抗进行测量，在试验测试中，阻抗测量采用单点测试 10 次取平均值的方式来降低测量误差。

（1）测试频率与探头宽度对探头阻抗的影响

为了分析探头阻抗特性受测试频率与探头宽度变化的影响，在探头直径及厚度确定的前提下，本文选取探头宽度为 2.0、2.5、3.0、3.5 cm 的铜环电极在不同频率下（30、100、200、300 MHz）检测探头阻抗随土壤含水率的变化情况。最终得到 112 组数据，使用正交法与探头阻抗 Z_p 进行多项式拟合，拟合结果如图 6、表 1 所示。

从图 6、表 1 中可以看出，环形电极结构固定时，环形电极的阻抗随着频率的增加而增加。工作频率固定时，其阻抗与铜环电极的宽度呈正相关关系。在工作频率为 100 MHz 时，环形探头每增宽 0.5 cm，其阻抗约增大 8 Ω。拟合曲线结果表明，其决定系数 R^2 均大于 0.95。但频率为 30 MHz 时，拟合曲线不单调，表明土壤含水率与探头阻抗不是单值关系，将无法通过探头阻抗直接获取土壤含水率。而频率达到 30 MHz 时，环形探头阻抗出现了容性与感性的相互转化，这一特点也将导致无法通过探头阻抗直接获取土壤含水率。进一步考虑到土壤在低频时受土壤电导率影响比较大[27]以及高频电子电路实现困难等因素，最终选 100 MHz 作为传感器的测试频率。

（2）土壤的介电常数对探头阻抗的影响

为了分析环形探头阻抗特性受土壤介电常数的影响，采用北京地区粘壤性土壤作为测试样本，配制成水分梯度从风干土到田间饱和持水量（体积含水率为 40% 左右）的测试样土。孙宇瑞等提出了一种利用四针结构驻波比原理的土壤水分传感器推算土壤介电常数的方法[28]。本文利用该方法选用北京

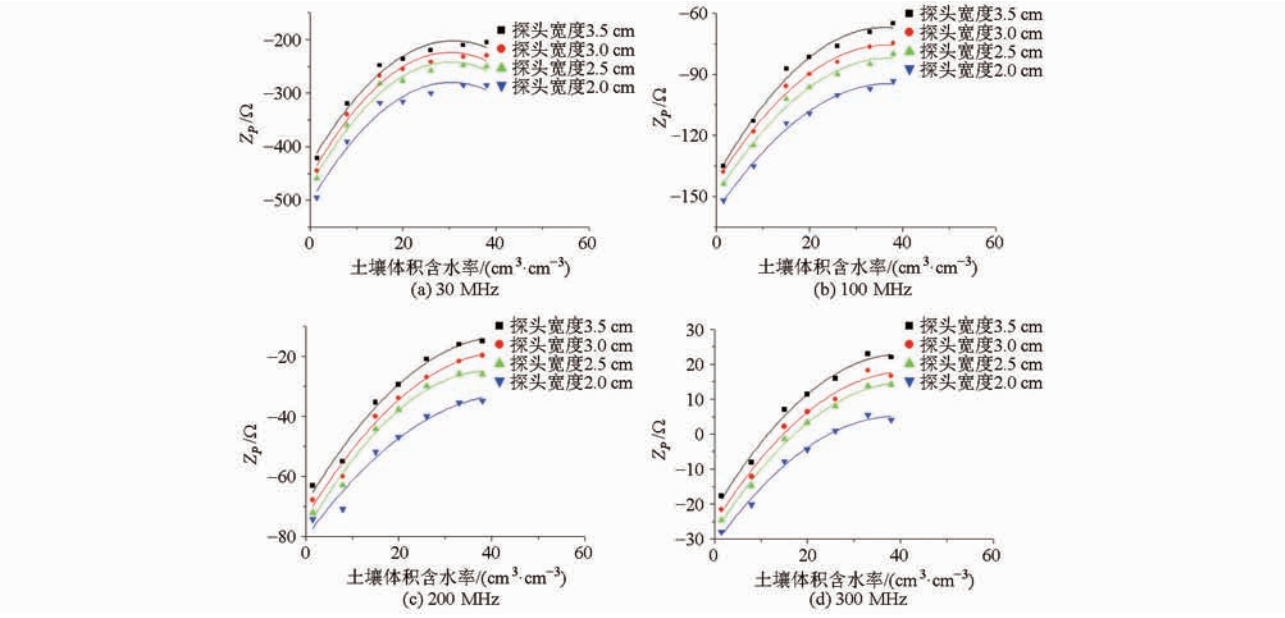

图 6 不同宽度环形探头在不同测试频率下的阻抗曲线

Fig. 6 Impedance curves of ring probe at different frequencies

表 1 不同宽度环形探头在不同测试频率下的阻抗拟合结果

Tab. 1 Impedance fitting results of ring probes with different widths at different frequencies

工作频率/MHz	电极宽度/cm	决定系数 R^2	多项式拟合结果
30	2.0	0.953 42	$y = -0.244x^2 + 14.826\,23x - 504.985\,43$
	2.5	0.969 26	$y = -0.256\,08x^2 + 15.420\,43x - 0.256\,08$
	3.0	0.969 42	$y = -0.257\,32x^2 + 15.518\,02x - 457.740\,57$
	3.5	0.971 13	$y = -0.243\,64x^2 + 15.022\,5x - 433.630\,69$
100	2.0	0.990 59	$y = -0.045\,24x^2 + 3.368\,84x - 2.157\,25$
	2.5	0.985 89	$y = -0.048\,16x^2 + 3.595\,9x - 149.066\,85$
	3.0	0.990 34	$y = -0.049\,78x^2 + 3.366\,464x - 143.068\,17$
	3.5	0.982 46	$y = -0.056\,25x^2 + 4.064\,1x - 140.411\,9$
200	2.0	0.951 21	$y = -0.023\,72x^2 + 2.127\,04x - 80.338\,76$
	2.5	0.980 44	$y = -0.034\,11x^2 + 2.694\,42x - 78.162\,48$
	3.0	0.976 71	$y = -0.029\,66x^2 + 2.558\,68x - 73.793\,34$
	3.5	0.977 53	$y = -0.030\,17x^2 + 2.593\,67x - 69.160\,17$
300	2.0	0.986 56	$y = -0.023\,8x^2 + 1.873\,08x - 31.690\,57$
	2.5	0.992 78	$y = -0.025\,09x^2 + 2.079\,08x - 28.247\,49$
	3.0	0.981 03	$y = -0.025\,26x^2 + 2.091\,23x - 25.382\,58$
	3.5	0.985 70	$y = -0.027\,30x^2 + 2.211\,9x - 21.845\,83$

林业大学自主研制的 BD-III 型土壤水分传感器对不同梯度的土壤含水率对应的介电常数进行推算[19],推算与 TOP 方程计算的对比结果如表 2 所示。由表 2 可以看出,试验推算结果与利用 TOP 方程计算结果有很好的相关性,由此说明试验推算结果能够比较正确地表现出土壤的介电特性。将推算结果与利用网络分析仪测量的探头阻抗值进行多项式拟合,其拟合结果如图 7 所示。其中探头宽度为 2.5 cm,工作频率为 100 MHz。

由图 7 的变化趋势可以看出,环形探头的端口阻抗 Z_p 与介电常数的变化呈严重的非线性关系。例如介电常数在 0 ~ 11 的区间内,曲线急剧上升,而

表 2 土壤介电常数对比

Tab. 2 Soil dielectric constants

介质	试验推算介电常数	TOP 方程计算介电常数
空气	1.00	1.00
体积含水率 2% 的土壤	2.40	2.63
体积含水率 9% 的土壤	5.50	5.42
体积含水率 16% 的土壤	9.10	8.58
体积含水率 22% 的土壤	10.61	11.69
体积含水率 27% 的土壤	15.02	14.62
体积含水率 30% 的土壤	17.30	16.54
体积含水率 35% 的土壤	21.80	20.36
体积含水率 39% 的土壤	25.10	23.89
水	81.00	81.00

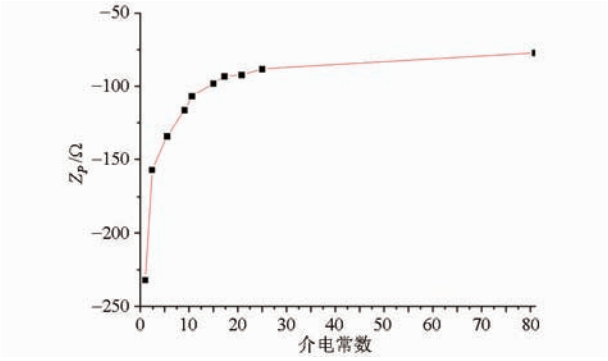

图 7　2.5 cm 环形探头在 100 MHz 频率下阻抗随介电常数变化的曲线

Fig. 7　Impedance curve with variation of dielectric constant of 2.5 cm ring probe at frequency of 100 MHz

后曲线变化明显减缓。测试土壤的饱和含水率对应的土壤的介电常数为 25.1，体积含水率约 2% 的干土介电常数约 2.4。介电常数在 2.4 ~ 25.1 之间时，探头的阻抗变化明显，因此该传感器探头能够满足粘壤性土质土壤体积含水率检测的需求。

2.2　环形探头电场分布状况

利用 HFSS 电磁场仿真软件建立环形探头的模型，设定求解频率为 100 MHz，集总端口激励方式，探头直径统一为 2.5 cm，宽度分别为 2.0、2.5、3.0、3.5 cm。设定周围填充介质的介电常数为 21（对应土壤体积含水率为 36%），PVC 安装管与铜环支架的介电常数为 4，管内介质设置为空气，介电常数为 1，设定铜环电极为理想电场边界，选取直径 12 cm、高度 13 cm 的圆柱体作为辐射边界条件。

由图 8 可以看出 4 种探头宽度的探头含水率检测区域主要在探头之间均匀分布，周围电场紧凑，没有出现分离现象。不同宽度的环形探头主要影响土壤监测区域电场分布的纵向范围与横向范围，图中淡绿色区域的电场强度为 104.9 V/m，其探头电场纵向达到淡绿色区域的电场强度的作用范围随着铜环宽度的增大而增大，依次为 9.5、10.0、10.5、11.0 cm。相反其探头电场横向达到淡绿色区域的电场强度的作用范围随着铜环宽度的增大而减少，依次为 10.5、10.0、9.5、9.0 cm。由上述现象可以得出，4 种宽度的环形电极都适用于作为传感器的检测探头，应用中可以通过对横向与纵向检测区域的综合考虑选取适当宽度的环形电极。考虑到农业检测中常规分层间隔为 10 cm，本文选取宽度为 2.5 cm 的铜环作为传感器电极。

由图 8 可知 PVC 管对电场强度有一定的衰减作用，铜环内部的电场强度要高于 PVC 管外土壤中的电场强度，考虑到铜环内部水分测试主板对电场分布的影响，本设计对水分测试主板进行了金属外壳屏蔽。

由以上可以看出：土壤水分传感器的阻抗与其探头宽度、测量频率及土壤介电常数有关，但完成系统结构设计后，前 2 个参数将不再变化，土壤水分传感器的阻抗只受土壤介电常数的影响。

3　传感器的性能测试

3.1　传感器动态响应性能试验

传感器的动态响应性能，主要表现为传感器检测区域含水率发生变化时，传感器完全响应所需要的时间，本次试验分 3 步进行。首先将传感器水分检测探头置于装有水的 PVC 测试筒的 PVC 测试管中，使用示波器测量得到传感器从刚通电到稳定输出所需要的时间为 1.28 ms。然后将传感器由测试筒中提出至空气中稳定输出的时间为 500 ms。最后将传感器再由空气中置于 PVC 测试管中，传感器达到稳定输出的时间为 480 ms。

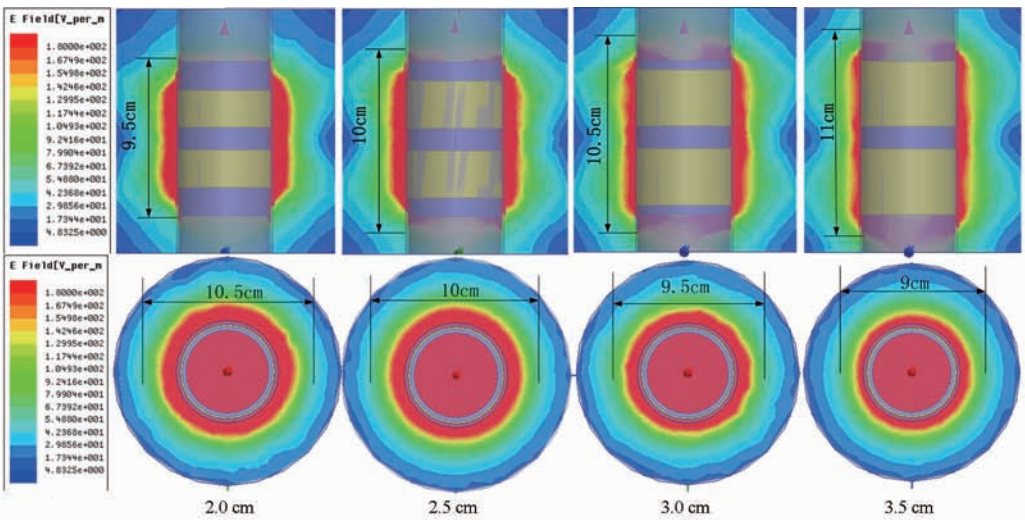

图 8　环形探头电场分布图

Fig. 8　Simulation of electrical field distribution of a ring probe

温度检测元件采用铠装铂电阻,其测温电路响应时间的原理和步骤与上述类似,经试验测得其动态响应时间分别为 38、720、800 ms。

3.2 温度传感器的标定试验及结果

温度传感器输出结果比较容易受到元器件精度的影响,所以在使用前需要对其进行标定。0℃以上部分采用北京博宇宝威实验设备有限公司的 SHP-450 型试验箱进行标定,其具体参数为恒温范围 0~60℃,精度 0.1℃。0℃以下部分采用青岛海尔集团 DW-40W255 型超低温保存箱(-40~0℃)进行标定。为了提高测量结果的准确度,将精度为 0.1℃的水银温度计作为参考温度分别设置在 2 个设备中。以 2℃为梯度,温度区间在 -20~40℃,经过升温、降温各一次取每个梯度的平均值,共测得 29 组数据,利用最小二乘法将采集处理后得到的温度与水银温度计的读取值进行拟合,其输出结果如图 9 所示。

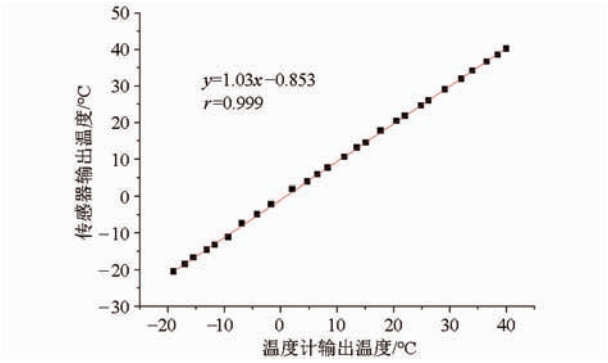

图 9 温度传感器的标定曲线

Fig. 9 Calibration curves of temperature sensor

由图 9 可以看出,其相关系数 r 达到了 0.999,自制的温度传感器的输出结果与水银温度计有显著的线性关系。

3.3 水分传感器的标定试验及结果

(1)传感器适应性与灵敏度试验验证

该试验在实验室环境下进行,环境温度为 25℃。选取 3 种不同质地组成的试验土壤:粘土、沙土与粘壤土,依据 2.1 节试验方法对 3 种土样进行处理,配制成水分梯度从风干土到田间饱和持水量的测试样土。因不同土质的饱和田间持水量不同,粘土与粘壤土在 2%~40% 内配置了 10 个梯度的体积含水率,而沙土在 2%~30% 配置了 8 个梯度的体积含水率。测量的数据为经过采集转换后得到的电压,对测得数据进行多项式拟合,结果如图 10 所示。

由图 10 可以看出,对于 3 种不同质地的土壤样本,传感器输出的结果与土壤体积含水率都具有良好的相关性,其决定系数 R^2 分别达到了 0.997 4、0.995 5、0.999 3。体积含水率每提高 10%,传感器输出电流经过采集转换后得到的电压都会有超过 100 mV的电压变化,说明传感器具有较好的灵敏性。

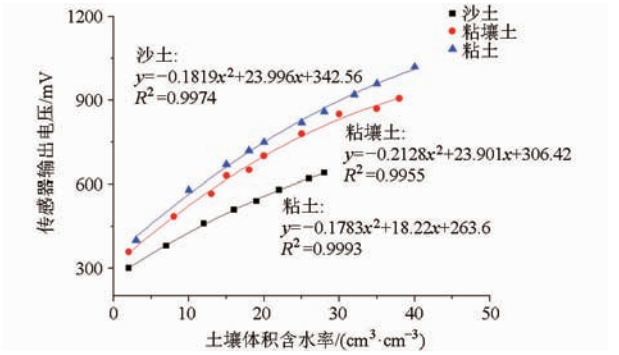

图 10 水分传感器标定曲线

Fig. 10 Calibration curves of moisture sensor

(2)温度影响的标定试验及补偿方式

温度对土壤介电特性与测量精度有显著影响[29]。采取有效方式对复合传感器的测量值的精度进行补偿是本次试验的重点研究内容。

选取 3 种不同质地组成的试验土壤:粘土、沙土与粘壤土,依据 2.1 节试验方法将每种质地的土壤配置成 4 种不同体积含水率的土壤样本。3 种土壤配比成的体积含水率分别为粘壤土:8%、15%、26%、37%;粘土:10%、18%、24%、39%;沙土:5%、10%、16%、25%;依次装入高 20 cm、直径 20 cm 的 4 个 PVC测试桶中(测试筒中心固定有高 20 cm、直径 5.6 cm 的 PVC 管)。使用保鲜膜密封静置 48 h,让土壤水分运移均衡。将本文研制的复合传感器探头置于土壤样本的 PVC 管中,然后用隔热棉将 PVC 管封死,以防止热量通过 PVC 管传入。将 PVC 测试筒置于烘干箱中。调节烘干箱温度使其在 25~50℃范围以 5℃为梯度变化。使用复合传感器探头自身的温度检测单元检测土壤温度,当其检测到的温度与烘干箱设置温度一致时,记录复合探头中水分检测单元的输出电压。依照上述方法,依次对另外 2 种质地的土壤样本进行测量,共测得 72 组数据。测试完毕后环刀取土,利用干燥法测得每种土样的含水率。试验结果如图 11、表 3 所示。

由图 11 可以看出,在 3 种土壤中复合传感器水分检测单元的输出电压随着土壤温度的升高均呈正相关关系。其主要原因在于温度的升高会加剧分子的极化程度与土壤中水分子的布朗运动,从而导致土壤的介电常数增大。此外环境温度的变化也会影响传感器中电子元器件的输出特性。基于上述现象表明,土壤温度的变化对复合传感器水分检测单元的输出具有一定的影响。

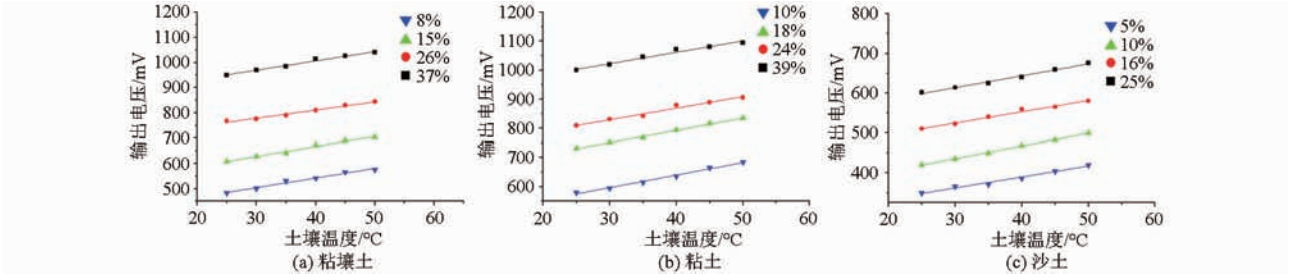

图 11　传感器输出电压与土壤温度的关系

Fig. 11　Relationship between sensor output voltage and soil temperature

表 3　决定系数拟合结果

Tab. 3　Fitting results of correlation coefficient

土壤类型	体积含水率/%	决定系数 R^2	线性拟合结果
粘壤土	8	0.982 3	$y=3.84x+388.67$
	15	0.988 5	$y=3.982\,9x+507.81$
	26	0.987 1	$y=3.24x+681.33$
	37	0.989 1	$y=3.691\,4x+858.9$
粘土	10	0.991 7	$y=4.32x+467.33$
	18	0.996 8	$y=4.205\,7x+624.95$
	24	0.977 2	$y=3.977\,1x+710.19$
	39	0.976 2	$y=3.914\,3x+905.38$
沙土	5	0.980 8	$y=2.754\,3x+279.71$
	10	0.998 3	$y=3.182\,9x+340.14$
	16	0.985 8	$y=2.845\,7x+439.29$
	25	0.988 5	$y=2.988\,6x+524.1$

为了消除环境温度对传感器输出的影响，利用 SPSS 软件对 3 种土壤所测数据进行线性回归分析，得到针对试验土壤的温度 T、土壤体积含水率 θ_v 与传感器输出电压 V_{out} 的关系模型如表 4 所示。

表 4　3 种土壤的线性回归模型

Tab. 4　Linear regression models of three kinds of soil

土壤类型	F 检验 p 值显著（$p=0.05$）	调整 R^2	线性回归模型
粘壤土	0	0.982 3	$V_{out}=1\,568.832\theta_v+3.689T+271.88$
粘土	0	0.991 7	$V_{out}=1\,112.562\theta_v+4.104T+448.889$
沙土	0	0.980 8	$V_{out}=1\,263.438\theta_v+2.943T+218.928$

由表 4 可以看出 3 种土质的 F 检验结果的 p 值显著为 0，在显著水平为 0.05 时，调整 R^2 均达到了 0.98 以上，说明上述建立的二元回归模型能很好地反映出传感器输出电压与土壤中的体积含水率和温度之间的关系。

3.4　复合传感器层间抗干扰性分析

为了消除传感器探头间相互干扰对传感器输出的影响，本文采用分时供电方式，即通过传感器采集主板控制同一时刻只有一个传感器探头供电测量。

试验对象为一个带 2 个检测探头的土壤剖面复合传感器。依据 2.1 节试验方法，制备体积含水率为 28% 的土壤样本。将传感器插入测试土壤中，调节上层探头的下边缘与下层探头的上边缘的间距，在 1 ~ 20 cm 范围内，以 1 cm 为步长，测量 2 个传感器探头水分检测单元的输出电压，其输出结果如图 12 所示。

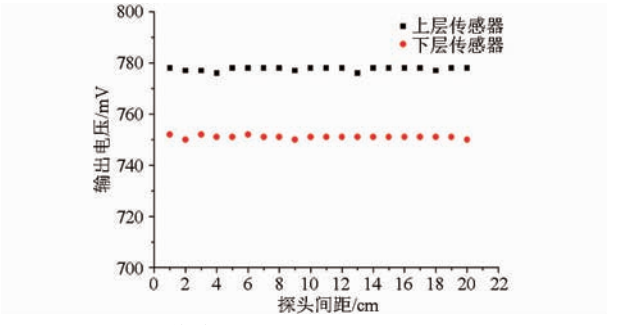

图 12　传感器输出电压与探头间距的关系

Fig. 12　Relationship between sensor output voltage and probe spacing

由图 12 可以看出，2 个传感器探头输出电压随着间距的变化，基本上不发生变化。主要因为采用分时供电策略，传感器探头间距对传感器输出电压基本没有影响。

4　田间动态测试

为了验证土壤复合传感器的可靠性与适应性，田间试验于 2014 年 3 月在北京市昌平区小汤山国家精准农业示范基地进行，试验区域为 1 m × 1 m × 2.5 m 的蒸渗仪，土壤为北京地区常见的粘壤土，试验区域种植冬小麦，PVC 测试管安装于蒸渗仪内。测试前首先从试验地区采集土样，利用 3.2 节方法对传感器进行标定。然后使用特定的安装工具打孔埋入长度为 1 m 的 PVC 测试管，尽量避免对检测土样的破坏，将测试土壤的扰动降至最小。复合传感器探头的安装深度分别为 30、60、90 cm。测试系统采用太阳能供电，数据采集间隔为 30 min。图 13 为测试环境图。

截取 2014 年 4 月 15—22 日的检测数据如图 14 所示，由图中可以看出土壤温度与体积含水率随时间呈连续周期变化。在浅层土壤（30 cm）处温度与体积含水率受昼夜环境变化影响比较大。同时，由于作物小麦正处于抽穗期，对水分需求比较大，进一

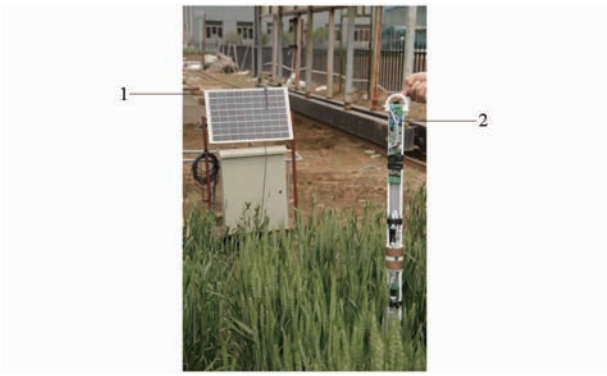

图 13 田间试验现场

Fig. 13 Field test site

1. 太阳能供电系统 2. 土壤剖面复合传感器

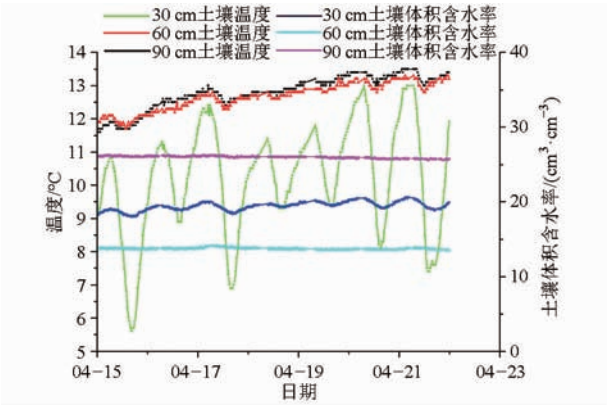

图 14 不同深度的土壤体积含水率与温度的动态变化曲线

Fig. 14 Dynamic change curves of soil moisture and temperature at different depths

步导致小麦根系区域(30 cm 处)土壤体积含水率的变化比较强烈。当作物根区水分缺少时,由于土壤毛细现象和作物根系吸附力的共同作用,深层土壤水分将不断补充给根区土壤,因此 60 cm 处的土壤体积含水率低于 30 cm 处土壤体积含水率。由于测试管体安装于蒸渗仪上,没有地下水源的补充,而 90 cm 处的土壤体积含水率低于田间饱和持水量,还不足以为 60 cm 处补充水分,所以 60 cm 处的土壤体积含水率较 90 cm 处的土壤体积含水率低。

本文所设计的土壤水分复合传感器并未考虑植物根区对传感器输出的影响。但在实际应用中,由于检测土壤中往往会分布很多植物根系,势必会对传感器的输出产生影响,可以通过建立水分传感器检测区域的根区密度与传感器输出的相应回归模型的方法对传感器进行校正。这也是本设计有待改进之处。

5 结论

(1)提出的土壤剖面复合传感器可实现对土壤剖面多层温度与土壤体积含水率的实时检测,对于植物根区土壤体积含水率与温度的检测及研究土壤水分、温度的运移都具有较大的意义。

(2)针对传感器测试频率与探头宽度进行了深入研究,借助网络矢量分析仪,对 4 种宽度的环形探头在不同梯度含水率的阻抗特性进行了分析,并通过 HFSS 电磁场仿真软件对环形电极的电场分布状态进行了仿真,最终确定传感器的测试探头为:直径为 5 cm、宽度为 2.5 cm、厚度为 0.09 cm 的铜环结构,测试频率为 100 MHz。

(3)从实验室标定与试验结果可以得出,设计的传感器具有较高的精度、适应性、灵敏度与动态响应性能。水分检测部分,复合传感器在 3 种不同质地土壤中试验证明,本文所设计的传感器具有较好的适应性,其多项式拟合决定系数分别为:粘土 0.997 4、粘壤土 0.995 5 与沙土 0.999 3。温度检测部分,对复合传感器温度检测单元的输出与测量值进行线性拟合,其相关系数达到了 0.999。

(4)通过试验分析了土壤温度与体积含水率对传感器输出的影响,利用统计回归方法建立了传感器在不同温度下的修正模型。

(5)持续的野外田间试验表明,土壤剖面复合传感器能够正确反映土壤剖面的温度与水分变化信息,具有较高的可靠性。

参 考 文 献

1 李连骏,孙宇瑞,林剑辉. 一种太阳能供电的土壤水分无线传感器[J]. 江苏大学学报:自然科学版,2009,30(6):541 - 544.
Li Lianjun, Sun Yurui, Lin Jianhui. A wireless-sensor for soil water content powered by solar energy[J]. Journal of Jiangsu University: Natural Science Edition, 2009, 30(6): 541 - 544. (in Chinese)

2 Kang S, Zhang J. Controlled alternate partial root-zone irrigation: its physiological consequences and impact on water use efficiency [J]. Journal of Experimental Botany, 2004, 407(55): 2437 - 2446.

3 Hutton R J, Loveys B R. A partial root zone drying irrigation strategy for citrus-effects on water use efficiency and fruit characteristics[J]. Agricultural Water Management, 2011, 98(10):1485 - 1496.

4 Hedley C B, Yule I J. A method for spatial prediction of daily soil water status for precise irrigation scheduling[J]. Agricultural Water Management, 2009, 96(12): 1737 - 1745.

5 Thompson R B, Gallardo M, Valdez L C, et al. Using plant water status to define threshold values for irrigation management of vegetable crops using soil moisture sensors[J]. Agricultural Water Management, 2007, 88(1 - 3):147 - 158.

6 Gao Xiaodong, Wu Pute, Zhao Xining, et al. Estimating the spatial means and variability of root-zone soil moisture in gullies using measurements from nearby uplands[J]. Journal of Hydrology, 2013, 476(1): 28 - 41.

7 Sheng W, Sun Y, Lammers P S, et al. Observing soil water dynamics under two field conditions by a novel sensor system[J]. Journal of Hydrology,2011,409(1-2):555-560.

8 李晓东,吴永烽,李光林,等.基于太阳能的无线土壤水分传感器的研制[J].农业工程学报,2010,26(11):13-18.
Li Xiaodong, Wu Yongfeng, Li Guanglin, et al. Development of wireless soil moisture sensor based on solar energy[J]. Transactions of the CSAE, 2010,26(11):13-18. (in Chinese)

9 赵燕东,马扬飞,王勇志.绿地精准灌溉控制系统设计与最优灌溉量分析[J].农业机械学报,2012,43(3):46-50.
Zhao Yandong, Ma Yangfei, Wang Yongzhi. Green land precision irrigation control system and analysis of optimal irrigation amount [J]. Translations of the Chinese Society for Agricultural Machinery, 2012, 43(3):46-50. (in Chinese)

10 Steven R, Robert C, Joaquin J, et al. Soil water sensing for water balance, ET and WUE[J]. Agricultural Water Management, 2012,104(2):1-9.

11 赵燕东,王一鸣. 智能化土壤水分分布速测系统[J]. 农业机械学报,2005,36(2):76-78.
Zhao Yandong, Wang Yiming. Intelligent system of measuring the spatial distributions of Soil moisture[J]. Transactions of the Chinese Society for Agricultural Machinery, 2005,36(2):76-78. (in Chinese)

12 彭曾愉,赵燕东.基于 μC/OS-Ⅱ操作系统的土壤水分实时监测系统[J]. 北京林业大学学报,2010,32(6):114-119.
Peng Zengyu, Zhao Yandong. A monitoring system of real-time soil water content based on μC/OS-Ⅱ operating system[J]. Journal of Beijing Forestry University, 2010,32(6):114-119. (in Chinese)

13 Dean T J, Bell J P, Baty A J B. Soil moisture measurement byan improved capacitance technique: part Ⅰ. sensor design andperformance[J]. Journal of Hydrology,1987, 93(1): 67-78.

14 Paltineanu I C, Starr J L. Real-time soil water dynamics using multi sensor capacitance probes: laboratory calibration[J]. Soil Science Society of America Journal,1997,61(6):1576-1585.

15 张学礼,胡振琪,初士立. 土壤含水量测定方法研究进展[J].土壤通报,2005,36(1):118-121.
Zhang Xueli, Hu Zhenqi, Chu Shili. Methods for measuring soil water content: a review[J]. Chinese Journal of Soil Science, 2005, 36(1): 118-121. (in Chinese)

16 蔡坤,岳学军,洪添胜,等.基于 RC 网络相频特性的土壤含水率传感器设计[J].农业工程学报,2013,29(7):36-43.
Cai Kun, Yue Xuejun, Hong Tiansheng, et al. Design of soil water content sensor based on phase-frequency characteristics of RC networks[J]. Transactions of the CSAE, 2013, 29(7): 36-43. (in Chinese)

17 Ortuani B, Benedetto A, Giudici M, et al, A Non-invasive approach to monitor variability of soil water content with electromagnetic methods[J]. Procedia Environmental Sciences, 2013(19): 446-455.

18 Cardenas-Lailhacar B, Dukes M D. Precision of soil moisture sensor irrigation controllers under field conditions[J]. Agricultural Water Management, 2010, 97(5): 666-672.

19 赵燕东,王一鸣. 基于驻波率原理的土壤含水率测量方法[J]. 农业机械学报,2002,33(4):109-111,121.
Zhao Yandong, Wang Yiming. Study on the measurement of soil water content based on the principle of standing-wave ratio[J]. Transactions of the Chinese Society for Agricultural Machinery, 2002,33(4):109-111,121. (in Chinese)

20 范寿康,卢春兰,李平辉. 微波技术与微波电路[M].北京:机械工业出版社,2003.

21 Hilhorst M A. Dielectric characterization of soil[D]. Wageningen:Wageningen Agricltural University, 1998.

22 Topp G C, Davis J L, Annan A P. Electromagnetic determination of soil water content: measurements in coaxial transmission lines[J]. Water Recourse Research, 1980, 16(3): 574-582.

23 何书森, 黄木梨. 微机在田间水层深度测试中的应用[J]. 农业机械学报, 1998,29(1):130-135.
He Shusen,Huang Muli. The application of micro-computer in the testing of field water depth[J]. Transactions of the Chinese Society for Agricultural Machinery, 1998, 29(1):130-135. (in Chinese)

24 张道辉, 赵红军, 周广芳,等. 农产品贮藏设施温控仪表温度漂移控制方法[J]. 农业机械学报, 2010,41(6):108-112.
Zhang Daohui, Zhao Hongjun, Zhou Guangfang,et al. Drift of the temperature-controlled instrument for the farm products storage [J]. Transactions of the Chinese Society for Agricultural Machinery,2010,41(6):108-112. (in Chinese)

25 赵燕东,聂铭君.双针结构土壤水分传感器探针最优长度分析与试验[J]. 农业机械学报,2011,42(11):39-43.
Zhao Yandong, Nie Mingjun. Optimal analysis for determining the dual-pin length of soil moisture probe[J]. Transactions of the Chinese Society for Agricultural Machinery, 2011,42(11):39-43. (in Chinese)

26 Ma Daokun,Sun Yurui,Wang Maohua, et al. Three-dimensional numerical modeling of a four-pin probe for soil water content[J]. Australian Journal of Soil Research, 2006,44(2):183-189.

27 赵燕东.土壤水分快速测量方法及其应用技术研究[D].北京:中国农业大学, 2002.
Zhao Yandong. Study on fast-measurement of soil water content and application technology[D]. Beijing: China Agricultural University,2002. (in Chinese)

28 孙宇瑞,汪懋华,赵燕东.一种基于驻波比原理测量土壤介电常数的方法[J]. 农业工程学报,1999,15(2):43-47.
Sun Yurui, Wang Maohua, Zhao Yandong. A kind of determinations of soil dielectric constant using the principle of standing-wave ratio[J]. Transactions of the CSAE, 1999,15 (2):43-47. (in Chinese)

29 郭文川,张鹏,宋克鑫,等.塿土介电特性与水分检测频率及温度影响[J].排灌机械学报,2013,31(8):713-718.
Guo Wenchuan, Zhang Peng, Song Kexin, et al. Dielectric properties of Lou soil and moisture content detection affected by frequency and temperature[J]. Journal of Drainage and Irrigation Machinery Engineering,2013,31(8):713-718. (in Chinese)